SIAM J. SCI. COMPUT.
Vol. 44, No. 6, pp. A3515–A3535
© 2022 Society for Industrial and Applied Mathematics

Downloaded 11/09/22 to 79.42.246.227 . Redistribution subject to SIAM license or copyright; see https://epubs.siam.org/terms-privacy

CONSTRUCTION AND EVALUATION OF PYTHAGOREAN HODOGRAPH CURVES IN EXPONENTIAL-POLYNOMIAL SPACES*

LUCIA ROMANI† AND ALBERTO VISCARDI‡

Abstract. In the past few decades polynomial curves with Pythagorean hodograph (PH curves) have received considerable attention due to their usefulness in various CAD/CAM areas, manufacturing, numerical control machining, and robotics. This work deals with classes of PH curves built upon exponential-polynomial spaces (EPH curves). In particular, for the two most frequently encountered exponential-polynomial spaces, we first provide necessary and sufficient conditions to be satisfied by the control polygon of the Bézier-like curve in order to fulfill the PH property. Then, for such EPH curves, fundamental characteristics like parametric speed or arc length are discussed to show the interesting analogies with their well-known polynomial counterparts. Differences and advantages with respect to ordinary PH curves become commendable when discussing the solutions to application problems like the interpolation of first-order Hermite data. Finally, a new evaluation algorithm for EPH curves is proposed and shown to compare favorably with the celebrated de Casteljau–like algorithm and two recently proposed methods: Woźny and Chudy's algorithm and the dynamic evaluation procedure by Yang and Hong.

Key words. exponential-polynomial curves, B-basis, evaluation, stability, pythagorean hodograph

MSC codes. 65D17, 65D18, 65Y20

DOI. 10.1137/21M1455711

1. Introduction.

Ordinary polynomial curve segments with the Pythagorean-hodograph (PH) property have been extensively studied [3], and their construction has been satisfactorily extended also to spaces spanned by algebraic-trigonometric polynomials [2, 5, 6, 10, 11]. Although spaces spanned by algebraic-hyperbolic polynomials have close analogies with the ones spanned by algebraic-trigonometric polynomials (see section 2), on the one hand they offer complementary solutions and, on the other hand, their handling might require some additional caution which is important to underline. Indeed, in the remainder of this manuscript we first show (see sections 3 and 4) that the constraints to be satisfied by the control points of the algebraic-hyperbolic Bézier curve segments in order to achieve the PH property mimic very closely the necessary and sufficient conditions known in the polynomial and algebraic-trigonometric cases. In addition, the computed expressions for their fundamental characteristics (parametric speed or arc length) seem to be very similar. But, when used in application contexts like interpolating C^1 Hermite data (see section 5), algebraic-hyperbolic Bézier curves allow one to get regular curves without undesired loops or self-intersections, whose shapes differ from those achievable by means of algebraic-trigonometric Bézier curves. For instance, when considering the planar Hermite data of Figure 1, none of the four solutions (see [3, Chapter 25]) provided by the ordinary polynomial PH quintics are free of loops. Instead, when the

*Submitted to the journal's Methods and Algorithms for Scientific Computing section October 27, 2021; accepted for publication (in revised form) August 16, 2022; published electronically November 9, 2022.

https://doi.org/10.1137/21M1455711

Funding: This work was supported by INdAM-GNCS 2020 project "Interpolation and smoothing: theoretical, computational and applied aspects" (Prot. U-UFMBAZ-2020-000564).

†AM^2 - Dipartimento di Matematica, Alma Mater Studiorum Università di Bologna, Bologna, Italy (lucia.romani@unibo.it).

‡Dipartimento di Matematica "Giuseppe Peano", Università di Torino, Torino, Italy (alberto.viscardi@unito.it).

Copyright © by SIAM. Unauthorized reproduction of this article is prohibited.

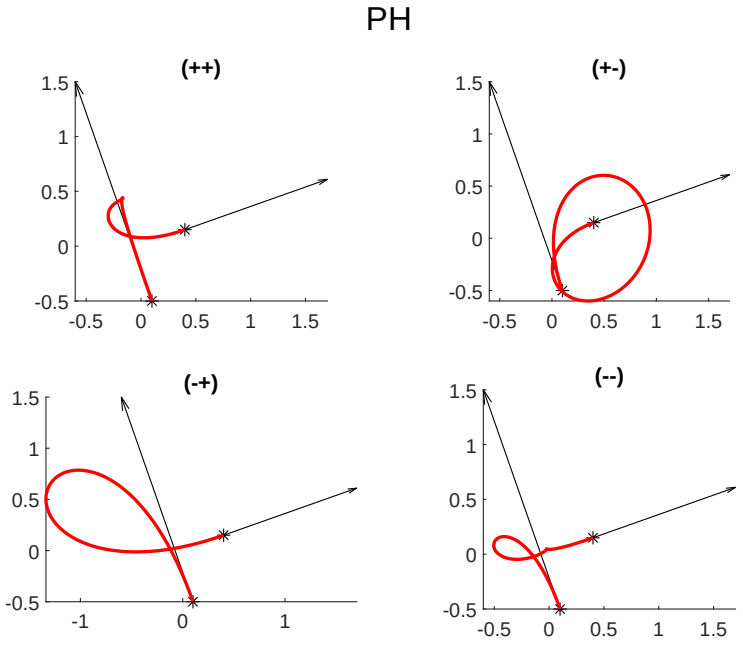

FIG. 1. *The four planar PH interpolants to the points* $\mathbf{r}_0 = (0.1, -0.5)$, $\mathbf{r}_5 = (0.4, 0.15)$ *and associated first derivatives* $\mathbf{d}_i = (-3.5, 10)$, $\mathbf{d}_f = (6.5, 2.3)$ *(here plotted with a scale factor of* $1/5$ *to fit into the picture). As for the meaning of the notation* $++$, $+-$, $-+$, $--$ *the reader can consult* [3, Chapter 25].

same Hermite problem is solved by using either algebraic-trigonometric PH (ATPH) curves or algebraic-hyperbolic PH (EPH) curves, for suitable choices of the free parameter (which both families are equipped with) several good solutions exist (see Figure 2). The further advantage offered by EPH curves is shown in Figure 3: when the C^1 Hermite data are sampled from some hyperbolic functions, then the EPH Hermite interpolant is able to reconstruct such functions exactly (similar to what ATPH curves do in the trigonometric case). These are of course practical reasons that motivate the study of EPH curves.

An additional reason that prompted us to investigate algebraic-hyperbolic PH curves arises from the observation that even if the hyperbolic cosine and sine are just the opposite side of the exponential coin from the trigonometric cosine and sine, the normalized B-basis (also known as Chebyshevian Bernstein basis) of the underlying extended Chebyshev space is known to be affected by numerical instability when large exponential shape parameters are selected [12]. Thus, one of the main goals of this work is also to suggest a stable formulation of the normalized B-basis of the two exponential-polynomial spaces (or, more precisely, algebraic-hyperbolic spaces) that are most frequently encountered when working with nonpolynomial PH curves, so that numerical instabilities are avoided. Furthermore, for such spaces, we aim at proposing a novel evaluation algorithm that is stable for a wide range of the exponential shape parameter, in contrast to the dynamic evaluation procedure in [15], and has a lower computational time (see section 6), compared with the de Casteljau–like B-algorithm [1, 7, 8, 9] (analogue of the de Casteljau algorithm for classical polynomial Bézier curves), and with the algorithm introduced by Woźny and Chudy in [13].

2. PH curves in exponential-polynomial spaces: EPH curves. Let $m \in \mathbb{N}_0$ and $\omega \in \mathbb{R}^+$, where $\mathbb{N}_0 = \mathbb{N} \cup \{0\}$ and $\mathbb{R}^+$ denotes the set of positive real numbers.

Copyright © by SIAM. Unauthorized reproduction of this article is prohibited.

Downloaded 11/09/22 to 79.42.246.227 . Redistribution subject to SIAM license or copyright; see https://epubs.siam.org/terms-privacy

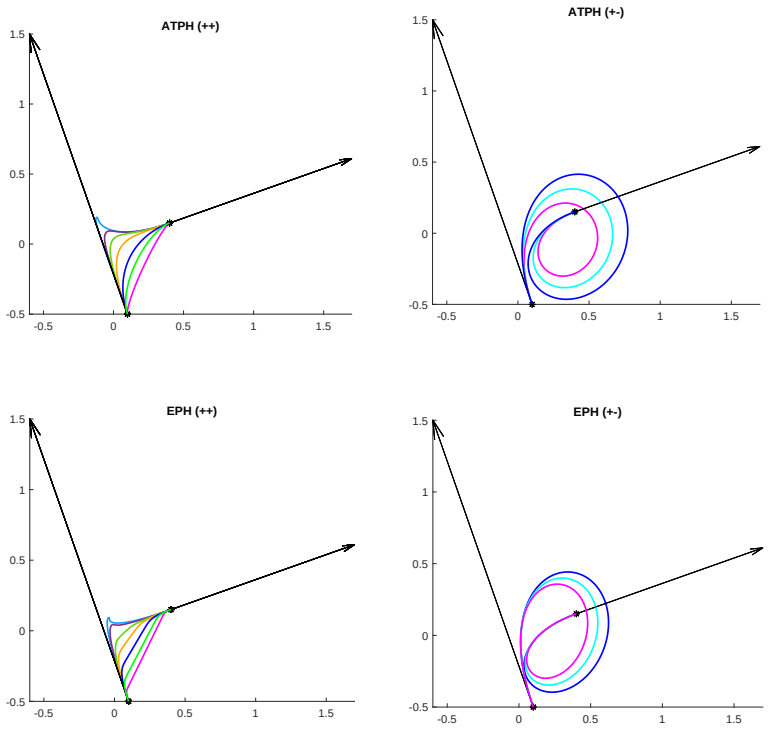

FIG. 2. *Top: Planar ATPH interpolants (see* [11]*) to the same Hermite data of Figure* 1. *Precisely, on the left the solution ++ obtained with shape parameter* $\alpha \in \{0.01, 0.05, 0.1, 0.2, 0.3, 0.4, 0.6\}$ *and on the right the solution +− obtained with shape parameter* $\alpha \in \{0.6, 0.7, 0.8\}$. *Bottom: Planar EPH interpolants to the same Hermite data of Figure* 1. *Precisely, on the left the solution ++ obtained with the exponential shape parameter* $\omega \in \{8, 10, 15, 20, 30, 50, 100\}$ *and on the right the solution +− obtained with the exponential shape parameter* $\omega \in \{3, 3.5, 4\}$. *As for the meaning of the notation ++, +− the reader can consult* [11] *and section* 5, *respectively.*

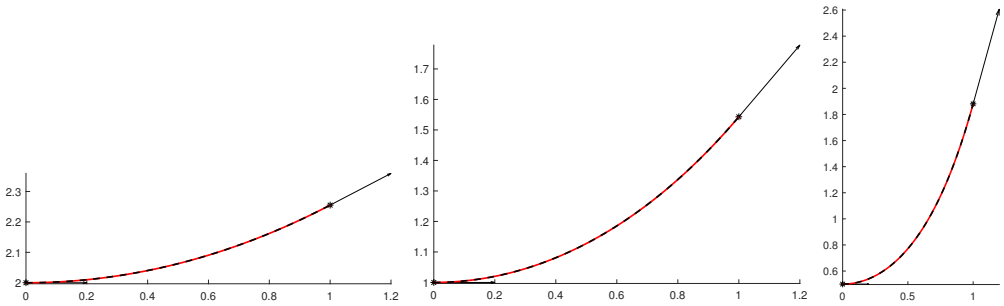

FIG. 3. *Planar EPH Hermite interpolant (solution ++) to the points* $\mathbf{r}_0 = (0, (2\omega)^{-1})$, $\mathbf{r}_5 = (1, (2\omega)^{-1}\cosh(2\omega))$ *and associated first derivatives* $\mathbf{d}_i = (1, 0)$, $\mathbf{d}_f = (1, \sinh(2\omega))$ *(here plotted with a scale factor of* $1/5$ *to fit into the picture), overlapping the function* $(2\omega)^{-1}\cosh(2\omega t)$, $t \in [0, 1]$, *for the following choices of the exponential shape parameter:* $\omega = 0.25$ *(left),* $\omega = 0.5$ *(center),* $\omega = 1$ *(right).*

DEFINITION 2.1 (exponential-polynomial spaces). *We define, in terms of* m *and* ω, *the following spaces of exponential polynomials:*

$$\mathcal{EP}_m^\omega := span\left\{ \{1, t\} \cup \bigcup_{k=1}^{m} \{e^{k\omega t}, e^{-k\omega t}\} \right\}$$

Copyright © by SIAM. Unauthorized reproduction of this article is prohibited.

Downloaded 11/09/22 to 79.42.246.227 . Redistribution subject to SIAM license or copyright; see https://epubs.siam.org/terms-privacy

and

$$\mathcal{OEP}_m^\omega \;:=\; span\left\{\; \{1,t\} \;\cup\; \bigcup_{k=1}^{m} \{e^{(2k-1)\omega t}, e^{-(2k-1)\omega t}\} \;\right\}.$$

We observe that

$$\mathcal{OEP}_0^\omega \;=\; \mathcal{EP}_0^\omega \;=\; span\,\{1,t\}\,, \qquad \mathcal{OEP}_1^\omega \;=\; \mathcal{EP}_1^\omega \;=\; span\left\{1,t,e^{\omega t},e^{-\omega t}\right\},$$

but, for $m > 1$, $\mathcal{OEP}_m^\omega \subsetneq \mathcal{EP}_{2m-1}^\omega$. Moreover, denoting with $\mathcal{D}$ the differential operator d/dt, it is easy to check that

$$\mathcal{DEP}_m^\omega \;=\; span\left\{\; \{1\} \;\cup\; \bigcup_{k=1}^{m} \{e^{k\omega t}, e^{-k\omega t}\} \;\right\} \;\subset\; \mathcal{EP}_m^\omega,$$

$$\mathcal{D}^2\mathcal{EP}_m^\omega \;=\; span\left\{\; \bigcup_{k=1}^{m} \{e^{k\omega t}, e^{-k\omega t}\} \;\right\} \;\subset\; \mathcal{DEP}_m^\omega,$$

and similarly

$$\mathcal{DOEP}_m^\omega \;=\; span\left\{\; \{1\} \;\cup\; \bigcup_{k=1}^{m} \{e^{(2k-1)\omega t}, e^{-(2k-1)\omega t}\} \;\right\} \;\subset\; \mathcal{OEP}_m^\omega,$$

$$\mathcal{D}^2\mathcal{OEP}_m^\omega \;=\; span\left\{\; \bigcup_{k=1}^{m} \{e^{(2k-1)\omega t}, e^{-(2k-1)\omega t}\} \;\right\} \;\subset\; \mathcal{DOEP}_m^\omega.$$

Again, we observe that

$$\mathcal{DOEP}_0^\omega \;=\; \mathcal{DEP}_0^\omega \;=\; span\,\{1\}\,, \qquad \mathcal{DOEP}_1^\omega \;=\; \mathcal{DEP}_1^\omega \;=\; span\left\{1,\; e^{\omega t},\; e^{-\omega t}\right\},$$

$$\mathcal{D}^2\mathcal{OEP}_0^\omega \;=\; \mathcal{D}^2\mathcal{EP}_0^\omega \;=\; \{0\}\,, \qquad \mathcal{D}^2\mathcal{OEP}_1^\omega \;=\; \mathcal{D}^2\mathcal{EP}_1^\omega \;=\; span\left\{e^{\omega t},\; e^{-\omega t}\right\},$$

but, for $m > 1$, $\mathcal{DOEP}_m^\omega \subsetneq \mathcal{DEP}_{2m-1}^\omega$ and $\mathcal{D}^2\mathcal{OEP}_m^\omega \subsetneq \mathcal{D}^2\mathcal{EP}_{2m-1}^\omega$.

DEFINITION 2.2 (PH curve in $\mathcal{EP}_m^\omega$). *A parametric curve* $\mathbf{r} : [0,1] \to \mathbb{R}^d$, $d \in \{2,3\}$, *is called a PH curve in* $\mathcal{EP}_m^\omega$ *if and only if one of the following holds:*

- *(planar EPH curve)* $d = 2$, $\mathbf{r}(t) = (x(t), y(t))$, $x, y \in \mathcal{EP}_m^\omega$, *with*

$$\left\{\begin{array}{l} x'(t) \;=\; (a_1(t))^2 \;-\; (a_2(t))^2\,, \\ y'(t) \;=\; 2a_1(t)a_2(t), \end{array}\right. \tag{2.1}$$

  for some exponential polynomials a_1, a_2.
- *(spatial EPH curve)* $d = 3$, $\mathbf{r}(t) = (x(t), y(t), z(t))$, $x, y, z \in \mathcal{EP}_m^\omega$, *with*

$$\left\{\begin{array}{l} x'(t) \;=\; (a_0(t))^2 \;+\; (a_1(t))^2 \;-\; (a_2(t))^2 \;-\; (a_3(t))^2\,, \\ y'(t) \;=\; 2\,(\; a_1(t)a_2(t) \;+\; a_0(t)a_3(t)\;)\,, \\ z'(t) \;=\; 2\,(\; a_1(t)a_3(t) \;-\; a_0(t)a_2(t)\;)\,, \end{array}\right. \tag{2.2}$$

  for some exponential polynomials a_0, a_1, a_2, a_3.

Remark 2.3. The curves defined via (2.1) and (2.2) are regular if and only if the exponential polynomials a_k do not have a common root in $[0,1]$ (see, e.g., [3]).

Copyright © by SIAM. Unauthorized reproduction of this article is prohibited.

Downloaded 11/09/22 to 79.42.246.227 . Redistribution subject to SIAM license or copyright; see https://epubs.siam.org/terms-privacy

Downloaded 11/09/22 to 79.42.246.227 . Redistribution subject to SIAM license or copyright; see https://epubs.siam.org/terms-privacy

In what follows we only consider the case $d = 3$, i.e., spatial curves: planar curves ($d = 2$) can be easily obtained setting $a_0(t) = a_3(t) = 0$ since this condition and (2.2) imply (2.1) along with $z(t)$ being constant. From (2.2) then, it is easy to get

$$(x'(t))^2 \,+\, (y'(t))^2 \,+\, (z'(t))^2 \,=\, \Big(\, (a_0(t))^2 \,+\, (a_1(t))^2 \,+\, (a_2(t))^2 \,+\, (a_3(t))^2 \,\Big)^2 .$$

Thus, the defining characteristic of a PH curve in $\mathcal{EP}^{\omega}_m$ is the fact that the coordinate components of its derivative (or hodograph) comprise a Pythagorean d-tuple of functions in $\mathcal{DEP}^{\omega}_m$—i.e., the sum of their squares coincides with the perfect square of a function in $\mathcal{DEP}^{\omega}_m$. By virtue of this remarkable property, the parametric speed of the curve $\sigma(t) = |\mathbf{r}'(t)|$ satisfies

$$\sigma(t) \,=\, (a_0(t))^2 \,+\, (a_1(t))^2 \,+\, (a_2(t))^2 \,+\, (a_3(t))^2 .$$

Clearly, a plethora of combinations of exponential polynomials a_k exists so that (2.1) and (2.2) identify PH curves in $\mathcal{EP}^{\omega}_m$. In order to simplify both the analysis and the construction, it is easier to identify spaces so that for every choice of the exponential polynomials a_k belonging to such spaces we can guarantee the resulting curves to be PH curves in $\mathcal{EP}^{\omega}_m$.

PROPOSITION 2.4. *Let $\mathcal{A}^{\omega}_m$ be either $\mathcal{DEP}^{\omega}_{\lfloor m/2\rfloor}$ or $\mathcal{D}^2\mathcal{OEP}^{\omega/2}_{\lfloor (m+1)/2\rfloor}$. Then, for every a_0, a_1, a_2, $a_3 \in \mathcal{A}^{\omega}_m$, (2.2) defines a PH curve in $\mathcal{EP}^{\omega}_m$.*

Proof. From (2.2), since $\mathcal{DEP}^{\omega}_m$ is a linear space, we only need to prove that

$$\Big(\mathcal{DEP}^{\omega}_{\lfloor m/2\rfloor}\Big)^2 \,\subseteq\, \mathcal{DEP}^{\omega}_m \qquad \text{and} \qquad \Big(\mathcal{D}^2\mathcal{OEP}^{\omega/2}_{\lfloor (m+1)/2\rfloor}\Big)^2 \,\subseteq\, \mathcal{DEP}^{\omega}_m .$$

Consider then, for α_k, $\beta_k \in \mathbb{R}$, $k = -\lfloor m/2\rfloor, \ldots, \lfloor m/2\rfloor$,

$$\sum_{k=-\lfloor m/2\rfloor}^{\lfloor m/2\rfloor} \alpha_k e^{k\omega t}, \sum_{k=-\lfloor m/2\rfloor}^{\lfloor m/2\rfloor} \beta_k e^{k\omega t} \,\in\, \mathcal{DEP}^{\omega}_{\lfloor m/2\rfloor}.$$

We have

$$\left(\sum_{k=-\lfloor m/2\rfloor}^{\lfloor m/2\rfloor} \alpha_k e^{k\omega t}\right)\left(\sum_{k=-\lfloor m/2\rfloor}^{\lfloor m/2\rfloor} \beta_k e^{k\omega t}\right) = \sum_{j,k=-\lfloor m/2\rfloor}^{\lfloor m/2\rfloor} \alpha_j\beta_k e^{(j+k)\omega t} \in \mathcal{DEP}^{\omega}_m,$$

since $-m \le -2\lfloor m/2\rfloor \le j + k \le 2\lfloor m/2\rfloor \le m$.

Similarly, for α_k, $\beta_k \in \mathbb{R}$, $k = 1 - \lfloor (m+1)/2\rfloor, \ldots, \lfloor (m+1)/2\rfloor$, and

$$\sum_{k=1-\lfloor (m+1)/2\rfloor}^{\lfloor (m+1)/2\rfloor} \alpha_k e^{\frac{2k-1}{2}\omega t}, \sum_{k=1-\lfloor (m+1)/2\rfloor}^{\lfloor (m+1)/2\rfloor} \beta_k e^{\frac{2k-1}{2}\omega t} \,\in\, \mathcal{D}^2\mathcal{OEP}^{\omega/2}_{\lfloor (m+1)/2\rfloor},$$

we have

$$\left(\sum_{k=1-\lfloor (m+1)/2\rfloor}^{\lfloor (m+1)/2\rfloor} \alpha_k e^{\frac{2k-1}{2}\omega t}\right)\left(\sum_{k=1-\lfloor (m+1)/2\rfloor}^{\lfloor (m+1)/2\rfloor} \beta_k e^{\frac{2k-1}{2}\omega t}\right)$$
$$= \sum_{j,k=1-\lfloor (m+1)/2\rfloor}^{\lfloor (m+1)/2\rfloor} \alpha_j\beta_k e^{(j+k-1)\omega t} \,\in\, \mathcal{DEP}^{\omega}_m,$$

since $-m \le 1 - 2\lfloor (m+1)/2\rfloor \le j + k - 1 \le 2\lfloor (m+1)/2\rfloor - 1 \le m$. ∎

Copyright © by SIAM. Unauthorized reproduction of this article is prohibited.

Downloaded 11/09/22 to 79.42.246.227 . Redistribution subject to SIAM license or copyright; see https://epubs.siam.org/terms-privacy

Examples of major interest that we consider are the following:

- $m = 1$: $\mathbf{r}(t)$ is a PH curve in $\mathcal{EP}_1^\omega = span\{1, t, e^{\omega t}, e^{-\omega t}\}$, its hodograph $\mathbf{r}'(t)$ is in $\mathcal{DEP}_1^\omega = span\{1, e^{\omega t}, e^{-\omega t}\}$, and $\mathcal{A}_1^\omega$ is either $\mathcal{DEP}_0^\omega = span\{1\}$ or $\mathcal{D}^2\mathcal{OEP}_1^{\omega/2} = span\{e^{\omega t/2}, e^{-\omega t/2}\}$;
- $m = 2$: $\mathbf{r}(t)$ is a PH curve in $\mathcal{EP}_2^\omega = span\{1, t, e^{\omega t}, e^{-\omega t}, e^{2\omega t}, e^{-2\omega t}\}$, its hodograph $\mathbf{r}'(t)$ is in $\mathcal{DEP}_2^\omega = span\{1, e^{\omega t}, e^{-\omega t}, e^{2\omega t}, e^{-2\omega t}\}$, and $\mathcal{A}_2^\omega$ is either $\mathcal{DEP}_1^\omega = span\{1, e^{\omega t}, e^{-\omega t}\}$ or $\mathcal{D}^2\mathcal{OEP}_1^{\omega/2} = span\{e^{\omega t/2}, e^{-\omega t/2}\}$.

For $m = 1$, $\mathcal{A}_1^\omega = \mathcal{DEP}_0^\omega$ corresponds to trivial line segments. Similarly, for $m = 2$, $\mathcal{A}_2^\omega = \mathcal{D}^2\mathcal{OEP}_1^{\omega/2}$ leads to PH curves in $\mathcal{EP}_1^\omega \subsetneq \mathcal{EP}_2^\omega$. In general, for m odd, $\mathcal{A}_m^\omega = \mathcal{DEP}_{\lfloor m/2 \rfloor}^\omega$ describes curves which actually live in $\mathcal{EP}_{m-1}^\omega$ while for m even, this is the case for $\mathcal{A}_m^\omega = \mathcal{D}^2\mathcal{OEP}_{\lfloor (m+1)/2 \rfloor}^{\omega/2}$. Therefore, from now on we only consider

$$\mathcal{A}_m^\omega := \begin{cases} \mathcal{DEP}_{m/2}^\omega & \text{if } m \text{ even}, \\ \mathcal{D}^2\mathcal{OEP}_{(m+1)/2}^{\omega/2} & \text{if } m \text{ odd}, \end{cases} \tag{2.3}$$

for which $\dim(\mathcal{A}_m^\omega) = m + 1$. Starting from $\{a_k\}_{k=0}^3$ in $\mathcal{A}_m^\omega$, (2.2) defines univocally $x'(t)$, $y'(t)$, and $z'(t)$ that belong to $\mathcal{DEP}_m^\omega$ and finally, by integration, one can obtain the analytic expressions of $x(t)$, $y(t)$, and $z(t)$ in $\mathcal{EP}_m^\omega$. Then, for a fixed m, three spaces need to be considered. For each of these spaces a B-basis (see [8]) is defined in what follows using the notation summarized in Table 1. According to Definition 2.2, Remark 2.3, Proposition 2.4, and (2.3), four functions a_0, a_1, a_2, a_3 in $\mathcal{A}_m^\omega$ having no common roots define a PH curve $\mathbf{r}(t) = (x(t), y(t), z(t))$ in $\mathcal{EP}_m^\omega$ as in (2.2). Such a curve can thus be associated to a function from the interval $[0, 1]$ to the quaternions in a natural way as follows.

Definition 2.5. *The function*

$$\mathbf{A}(t) := a_0(t) + a_1(t)\mathbf{i} + a_2(t)\mathbf{j} + a_3(t)\mathbf{k},$$

where $\mathbf{i}, \mathbf{j}, \mathbf{k}$ *denote the so-called fundamental quaternion units (see, e.g., [3, section 5.3]), is called the preimage of* $\mathbf{r}(t)$.

Expanding the coefficients of the preimage with respect to a B-basis of $\mathcal{A}_m^\omega$ as $a_k(t) = \sum_{j=0}^m a_{k,j}\psi_{j,m}^\omega(t)$, $k \in \{0, \dots, 3\}$, for some $a_{k,j} \in \mathbb{R}$, we can rewrite

$$\mathbf{A}(t) = \sum_{j=0}^m \mathbf{A}_j \psi_{j,m}^\omega(t), \qquad \text{where} \qquad \mathbf{A}_j = a_{0,j} + a_{1,j}\mathbf{i} + a_{2,j}\mathbf{j} + a_{3,j}\mathbf{k}. \tag{2.4}$$

Moreover, we can compactly write the hodograph $\mathbf{r}'(t) = (x'(t), y'(t), z'(t))$ of $\mathbf{r}(t)$ with the pure vector quaternion

$$\mathbf{r}'(t) = \mathbf{A}(t)\mathbf{i}\mathbf{A}^*(t). \tag{2.5}$$

Here and in the following, with an abuse of notation, we identify vectors in $\mathbb{R}^3$ and pure vector quaternions via the natural bijection $(x, y, z) \longleftrightarrow x\mathbf{i} + y\mathbf{j} + z\mathbf{k}$. Accordingly, in view of (2.5), the parametric speed of $\mathbf{r}(t)$ has the quaternionic representation

$$\sigma(t) = |\mathbf{r}'(t)| = |\mathbf{A}(t)\mathbf{i}\mathbf{A}^*(t)| = |\mathbf{A}(t)|^2 = \mathbf{A}(t)\mathbf{A}^*(t). \tag{2.6}$$

Table 1
Notation used for the exponential-polynomial spaces and their respective B-basis.

space	$\mathcal{A}_m^\omega$	$\mathcal{DEP}_m^\omega$	$\mathcal{EP}_m^\omega$
dimension	$m+1$	$2m+1$	$2(m+1)$
B-basis	$\{\psi_{j,m}^\omega\}_{j=0}^m$	$\{\varphi_{j,m}^\omega\}_{j=0}^{2m}$	$\{\phi_{j,m}^\omega\}_{j=0}^{2m+1}$

Copyright © by SIAM. Unauthorized reproduction of this article is prohibited.

Downloaded 11/09/22 to 79.42.246.227 . Redistribution subject to SIAM license or copyright; see https://epubs.siam.org/terms-privacy

3. PH curves in $\mathcal{EP}_1^\omega$.

3.1. The normalized B-basis of the space $\mathcal{EP}_1^\omega$. On the interval $[0,1]$ the nonnegative exponential functions

$$\begin{aligned}\psi_{0,1}^\omega(t) &= \frac{e^{\frac{\omega}{2}(1-t)}-e^{-\frac{\omega}{2}(1-t)}}{e^{\frac{\omega}{2}}-e^{-\frac{\omega}{2}}} = \frac{\sinh\left(\frac{\omega}{2}-\frac{\omega}{2}t\right)}{\sinh\left(\frac{\omega}{2}\right)},\\ \psi_{1,1}^\omega(t) &= \frac{e^{\frac{\omega}{2}t}-e^{-\frac{\omega}{2}t}}{e^{\frac{\omega}{2}}-e^{-\frac{\omega}{2}}} = \frac{\sinh\left(\frac{\omega}{2}t\right)}{\sinh\left(\frac{\omega}{2}\right)}\end{aligned} \tag{3.1}$$

define a B-basis of the extended Chebyshev space $\mathcal{A}_1^\omega = \mathcal{D}^2\mathcal{OEP}_1^{\omega/2} = span\{e^{\frac{\omega}{2}t}, e^{-\frac{\omega}{2}t}\}$. However, note that $\{\psi_{0,1}^\omega(t), \psi_{1,1}^\omega(t)\}$ is not normalized since $\psi_{0,1}^\omega(t)+\psi_{1,1}^\omega(t) \neq 1$ for $t \in (0,1)$. By squaring an arbitrary function $f \in \mathcal{A}_1^\omega$, we obtain a function f^2 that belongs to the exponential space $\mathcal{DEP}_1^\omega = span\{1, e^{\omega t}, e^{-\omega t}\}$. Since we assume $\omega \in \mathbb{R}^+$, $\mathcal{DEP}_1^\omega$ is an extended Chebyshev space that, on the interval $[0,1]$, admits a normalized B-basis of the form

$$\begin{aligned}\varphi_{0,1}^\omega(t) &= \frac{(e^{\omega(1-t)}-1)^2\, e^{\omega t}}{(e^\omega-1)^2} = \frac{\cosh(\omega-\omega t)-1}{\cosh(\omega)-1},\\ \varphi_{1,1}^\omega(t) &= \frac{(e^{-\omega t}-1)\,(e^{\omega t}-e^\omega)\,(e^\omega+1)}{(e^\omega-1)^2} = \frac{\cosh(\omega)-\cosh(\omega t)-\cosh(\omega-\omega t)+1}{\cosh(\omega)-1},\\ \varphi_{2,1}^\omega(t) &= \frac{(e^{\omega t}-1)^2\, e^{\omega(1-t)}}{(e^\omega-1)^2} = \frac{\cosh(\omega t)-1}{\cosh(\omega)-1}.\end{aligned} \tag{3.2}$$

The exponential functions $\{\varphi_{0,1}^\omega(t), \varphi_{1,1}^\omega(t), \varphi_{2,1}^\omega(t)\}$ satisfy the following relationships with the exponential functions $\{\psi_{0,1}^\omega(t), \psi_{1,1}^\omega(t)\}$:

$$\begin{aligned}&\left(\psi_{0,1}^\omega(t)\right)^2 = \varphi_{0,1}^\omega(t), \quad \psi_{0,1}^\omega(t)\psi_{1,1}^\omega(t) = \tfrac{1}{2}c_1(\omega)\varphi_{1,1}^\omega(t), \quad \left(\psi_{1,1}^\omega(t)\right)^2 = \varphi_{2,1}^\omega(t),\\ &\text{with} \quad c_1(\omega) = \frac{2}{e^{\frac{\omega}{2}}+e^{-\frac{\omega}{2}}} = \frac{1}{\cosh\left(\frac{\omega}{2}\right)}.\end{aligned} \tag{3.3}$$

The antiderivative of $f^2 \in \mathcal{DEP}_1^\omega$ is an exponential-polynomial function that belongs to the order-4 exponential-polynomial space $\mathcal{EP}_1^\omega = span\{1, t, e^{\omega t}, e^{-\omega t}\}$. The exponential-polynomial functions

$$\begin{aligned}\phi_{0,1}^\omega(t) &= \tfrac{e^{\omega(1-t)}-e^{-\omega(1-t)}-2\omega(1-t)}{e^\omega-e^{-\omega}-2\omega} = \tfrac{\sinh(\omega-\omega t)-\omega(1-t)}{\sinh(\omega)-\omega},\\ \phi_{1,1}^\omega(t) &= \tfrac{(e^{-\omega}-1)\left((\omega+1-e^\omega)e^{\omega t}+((\omega-1)e^\omega+1)e^{\omega(1-t)}\right)+(e^\omega-1)\left(\omega(2t+(e^{-\omega}+e^\omega)(1-t))+e^{-\omega}-e^\omega\right)}{(\omega+2+e^\omega(\omega-2))\,(e^\omega-e^{-\omega}-2\omega)}\\ &= \tfrac{-\omega t-\omega(1-t)\cosh(\omega)+\omega\cosh(\omega-\omega t)+\sinh(\omega)-\sinh(\omega t)-\sinh(\omega-\omega t)}{(\omega\coth(\frac{\omega}{2})-2)(\omega-\sinh(\omega))},\\ \phi_{2,1}^\omega(t) &= \tfrac{(e^{-\omega}-1)\left((\omega+1-e^\omega)e^{\omega(1-t)}+((\omega-1)e^\omega+1)e^{\omega t}\right)+(e^\omega-1)\left(\omega(2(1-t)+(e^{-\omega}+e^\omega)t)+e^{-\omega}-e^\omega\right)}{(\omega+2+e^\omega(\omega-2))\,(e^\omega-e^{-\omega}-2\omega)}\\ &= \tfrac{-\omega(1-t)-\omega t\cosh(\omega)+\omega\cosh(\omega t)+\sinh(\omega)-\sinh(\omega-\omega t)-\sinh(\omega t)}{(\omega\coth(\frac{\omega}{2})-2)(\omega-\sinh(\omega))},\\ \phi_{3,1}^\omega(t) &= \tfrac{e^{\omega t}-e^{-\omega t}-2\omega t}{e^\omega-e^{-\omega}-2\omega} = \tfrac{\sinh(\omega t)-\omega t}{\sinh(\omega)-\omega}\end{aligned} \tag{3.4}$$

define a normalized B-basis of the extended Chebyshev space $\mathcal{EP}_1^\omega$ on $[0,1]$. For later use we observe that for the antiderivatives of the basis functions of $\mathcal{DEP}_1^\omega$ we can write

Copyright © by SIAM. Unauthorized reproduction of this article is prohibited.

$$\int_0^t \varphi_{0,1}^{\omega}(x)dx = c_2(\omega)\sum_{i=1}^{3}\phi_{i,1}^{\omega}(t), \quad \int_0^t \varphi_{1,1}^{\omega}(x)dx = \frac{c_3(\omega)}{c_1(\omega)}\sum_{i=2}^{3}\phi_{i,1}^{\omega}(t), \tag{3.5}$$
$$\int_0^t \varphi_{2,1}^{\omega}(x)dx = c_2(\omega)\,\phi_{3,1}^{\omega}(t),$$

with

$$c_2(\omega) = \int_0^1 \varphi_{0,1}^{\omega}(t)\,dt = \frac{\sinh(\omega)-\omega}{\omega(\cosh(\omega)-1)}, \tag{3.6}$$
$$c_3(\omega) = c_1(\omega)\int_0^1 \varphi_{1,1}^{\omega}(t)\,dt = \frac{\frac{\omega}{2}\coth\left(\frac{\omega}{2}\right)-1}{\frac{\omega}{2}\sinh\left(\frac{\omega}{2}\right)}.$$

Remark 3.1. For all $\omega \in \mathbb{R}^+$, we always have $c_1(\omega), c_2(\omega), c_3(\omega) \neq 0$.

3.2. Geometric properties of Bézier-like curves in $\mathcal{EP}_1^{\omega}$.

DEFINITION 3.2 (Bézier-like curves in $\mathcal{EP}_1^{\omega}$). *Given a control polygon with vertices $\mathbf{r}_i \in \mathbb{R}^d$, $i = 0, \ldots, 3$, the associated Bézier-like curve in $\mathcal{EP}_1^{\omega}$ is defined as*

$$\mathbf{r}(t) = \sum_{i=0}^{3} \mathbf{r}_i\,\phi_{i,1}^{\omega}(t), \qquad t \in [0,1]. \tag{3.7}$$

PROPOSITION 3.3 (properties of Bézier-like curves in $\mathcal{EP}_1^{\omega}$). *The Bézier-like curve in* (3.7) *has the following properties:*

(a) Convex hull property and geometric invariance property. *The entire curve lies inside the convex hull of its control points and its shape is independent of the coordinate system, i.e., it is scale and translation invariant.*

(b) Symmetry. *The control points* $\mathbf{r}_0, \mathbf{r}_1, \mathbf{r}_2, \mathbf{r}_3$ *and* $\mathbf{r}_3, \mathbf{r}_2, \mathbf{r}_1, \mathbf{r}_0$ *define the same curve with respect to different parameterizations, i.e.,*

$$\sum_{i=0}^{3} \mathbf{r}_i\phi_{i,1}^{\omega}(t) = \sum_{i=0}^{3} \mathbf{r}_{3-i}\phi_{i,1}^{\omega}(1-t), \qquad t \in [0,1].$$

(c) Derivative formula.

$$\frac{d}{dt}\mathbf{r}(t) = \sum_{i=0}^{2} \frac{\Delta\mathbf{r}_i}{\int_0^1 \varphi_{i,1}^{\omega}(x)\,dx}\,\varphi_{i,1}^{\omega}(t), \qquad t \in [0,1],$$

where, for all $i = 0, 1, 2$, $\Delta\mathbf{r}_i = \mathbf{r}_{i+1} - \mathbf{r}_i$.

(d) Endpoint conditions.

$$\mathbf{r}(0) = \mathbf{r}_0, \qquad \mathbf{r}'(0) = \frac{1}{c_2(\omega)}(\mathbf{r}_1 - \mathbf{r}_0),$$

$$\mathbf{r}(1) = \mathbf{r}_3, \qquad \mathbf{r}'(1) = \frac{1}{c_2(\omega)}(\mathbf{r}_3 - \mathbf{r}_2).$$

Proof. See section SM1 for the proof. ∎

3.3. Control polygons of PH curves in $\mathcal{EP}_1^{\omega}$.

To construct a PH curve in $\mathcal{EP}_1^{\omega}$, the functions a_0, a_1, a_2, a_3 are chosen in $\mathcal{A}_1^{\omega}$ and thus

$$a_k(t) = a_{k,0}\psi_{0,1}^{\omega}(t) + a_{k,1}\psi_{1,1}^{\omega}(t), \qquad k \in \{0, \ldots, 3\},$$

Copyright © by SIAM. Unauthorized reproduction of this article is prohibited.

Downloaded 11/09/22 to 79.42.246.227 . Redistribution subject to SIAM license or copyright; see https://epubs.siam.org/terms-privacy

Downloaded 11/09/22 to 79.42.246.227 . Redistribution subject to SIAM license or copyright; see https://epubs.siam.org/terms-privacy

for some $a_{k,0}$, $a_{k,1} \in \mathbb{R}$. Consequently, the associated preimage is

$$\mathbf{A}(t) \;=\; \mathbf{A}_0\psi^{\omega}_{0,1}(t) \;+\; \mathbf{A}_1\psi^{\omega}_{1,1}(t), \tag{3.8}$$

where

$$\mathbf{A}_j \;=\; a_{0,j} \;+\; a_{1,j}\mathbf{i} \;+\; a_{2,j}\mathbf{j} \;+\; a_{3,j}\mathbf{k}, \qquad j \;=\; 0,\, 1. \tag{3.9}$$

PROPOSITION 3.4. *A PH curve* $\mathbf{r}(t)$ *in* $\mathcal{EP}^{\omega}_1$ *can be expressed in the Bézier-like form* $\mathbf{r}(t) = \sum_{i=0}^{3} \mathbf{r}_i \phi^{\omega}_{i,1}(t)$, *with Bézier-like control points* $\mathbf{r}_i$, $i = 1, \ldots, 3$, *given in terms of the freely chosen integration constant* $\mathbf{r}_0$, *of the numbers in* (3.6) *and of the coefficients of the preimage* $\mathbf{A}(t)$ *in* (3.8) *and* (3.9) *by*

$$\begin{aligned} \mathbf{r}_1 \;&=\; \mathbf{r}_0 \;+\; c_2(\omega)\,\mathbf{A}_0\mathbf{i}\mathbf{A}_0^*, \qquad \mathbf{r}_2 \;=\; \mathbf{r}_1 \;+\; c_3(\omega)\,\frac{1}{2}\,(\mathbf{A}_0\mathbf{i}\mathbf{A}_1^* + \mathbf{A}_1\mathbf{i}\mathbf{A}_0^*), \\ \mathbf{r}_3 \;&=\; \mathbf{r}_2 \;+\; c_2(\omega)\,\mathbf{A}_1\mathbf{i}\mathbf{A}_1^*. \end{aligned} \tag{3.10}$$

Proof. See section SM2 for the proof. ∎

Remark 3.5. Since, from (3.6), $\lim_{\omega\to 0} c_2(\omega) = \lim_{\omega\to 0} c_3(\omega) = 1/3$, (3.10) recovers the well-known results of the cubic polynomial case when $\omega \to 0$; (see [3]).

3.4. Parametric speed and arc length in $\mathcal{EP}^{\omega}_1$.

PROPOSITION 3.6. *The parametric speed of* $\mathbf{r}(t)$ *is a function in* $\mathcal{DEP}^{\omega}_1$ *with the explicit expression* $\sigma(t) = \sum_{i=0}^{2} \sigma_i \varphi^{\omega}_{i,1}(t)$, *where*

$$\sigma_0 \;=\; |\mathbf{A}_0|^2, \qquad \sigma_1 \;=\; c_1(\omega)\,\frac{1}{2}\,(\mathbf{A}_1\mathbf{A}_0^* + \mathbf{A}_0\mathbf{A}_1^*), \qquad \sigma_2 \;=\; |\mathbf{A}_1|^2. \tag{3.11}$$

Proof. See section SM3 for the proof. ∎

PROPOSITION 3.7. *The arc length function of* $\mathbf{r}(t)$ *is a function in* $\mathcal{EP}^{\omega}_1$ *having the expression* $s(t) = \sum_{i=0}^{3} s_i \phi^{\omega}_{i,1}(t)$, *where*

$$s_0 \;=\; 0, \qquad s_1 \;=\; s_0 + \sigma_0 c_2(\omega), \qquad s_2 \;=\; s_1 + \sigma_1 \frac{c_3(\omega)}{c_1(\omega)}, \qquad s_3 \;=\; s_2 + \sigma_2 c_2(\omega).$$

Proof. See section SM4 for the proof. ∎

COROLLARY 3.8. *The total arc length of* $\mathbf{r}(t)$ *is*

$$\begin{aligned} s(1) = s_3 \;&=\; (\sigma_0 + \sigma_2)\,c_2(\omega) \;+\; \sigma_1\,\frac{c_3(\omega)}{c_1(\omega)} \\ &= c_2(\omega)\,\left(|\mathbf{A}_0|^2 + |\mathbf{A}_1|^2\right) \;+\; c_3(\omega)\,\frac{1}{2}\,(\mathbf{A}_1\mathbf{A}_0^* + \mathbf{A}_0\mathbf{A}_1^*). \end{aligned} \tag{3.12}$$

Remark 3.9. When $\omega \to 0$, the total arc length formula in (3.12) yields $s(1) = \left(|\mathbf{A}_0|^2 + |\mathbf{A}_1|^2\right)/3 + (\mathbf{A}_1\mathbf{A}_0^* + \mathbf{A}_0\mathbf{A}_1^*)/6$, thus recovering the well-known result of the cubic polynomial case [3].

4. PH curves in $\mathcal{EP}^{\omega}_2$.

4.1. The normalized B-basis of the space $\mathcal{EP}^{\omega}_2$. By squaring an arbitrary function $f \in \mathcal{A}^{\omega}_2 = span\{1, e^{\omega t}, e^{-\omega t}\}$, we obtain a function f^2 that belongs to the exponential space $\mathcal{DEP}^{\omega}_2 = span\{1, e^{\omega t}, e^{-\omega t}, e^{2\omega t}, e^{-2\omega t}\}$. Since $\mathcal{A}^{\omega}_2 = \mathcal{DEP}^{\omega}_1$ we

Copyright © by SIAM. Unauthorized reproduction of this article is prohibited.

Downloaded 11/09/22 to 79.42.246.227 . Redistribution subject to SIAM license or copyright; see https://epubs.siam.org/terms-privacy

can choose $\psi^{\omega}_{j,2}(t) = \varphi^{\omega}_{j,1}(t)$, $j \in \{0,1,2\}$ as in (3.2). Then, $\mathcal{DEP}^{\omega}_2$ is an extended Chebyshev space that, on the interval $[0,1]$, admits a normalized B-basis of the form

$$\begin{aligned}
\varphi^{\omega}_{0,2}(t) &= \left(\psi^{\omega}_{0,2}(t)\right)^2, \qquad \varphi^{\omega}_{1,2}(t) = 2\psi^{\omega}_{0,2}(t)\psi^{\omega}_{1,2}(t),\\
\varphi^{\omega}_{2,2}(t) &= \left(\psi^{\omega}_{1,2}(t)\right)^2 + 2\psi^{\omega}_{0,2}(t)\psi^{\omega}_{2,2}(t),\\
\varphi^{\omega}_{3,2}(t) &= 2\psi^{\omega}_{1,2}(t)\psi^{\omega}_{2,2}(t), \qquad \varphi^{\omega}_{4,2}(t) = \left(\psi^{\omega}_{2,2}(t)\right)^2.
\end{aligned}$$

The inverse relationship between the exponential functions $\{\varphi^{\omega}_{j,2}(t)\}_{j=0}^{4}$ and the exponential functions $\{\psi^{\omega}_{j,2}(t)\}_{j=0}^{2}$ is instead given by

$$\begin{aligned}
\left(\psi^{\omega}_{0,2}(t)\right)^2 &= \varphi^{\omega}_{0,2}(t), \qquad \psi^{\omega}_{0,2}(t)\psi^{\omega}_{1,2}(t) = \frac{1}{2}\varphi^{\omega}_{1,2}(t),\\
\left(\psi^{\omega}_{1,2}(t)\right)^2 &= q_0(\omega)\varphi^{\omega}_{2,2}(t), \qquad \psi^{\omega}_{0,2}(t)\psi^{\omega}_{2,2}(t) = \frac{1}{2}q_1(\omega)\varphi^{\omega}_{2,2}(t),\\
\psi^{\omega}_{1,2}(t)\psi^{\omega}_{2,2}(t) &= \frac{1}{2}\varphi^{\omega}_{3,2}(t), \qquad \left(\psi^{\omega}_{2,2}(t)\right)^2 = \varphi^{\omega}_{4,2}(t),\\
\text{with} \qquad q_0(\omega) &= \frac{\cosh(\omega)+1}{\cosh(\omega)+2}, \qquad q_1(\omega) = \frac{1}{\cosh(\omega)+2}.
\end{aligned} \tag{4.1}$$

The antiderivative of a function in $\mathcal{DEP}^{\omega}_2$ is an exponential-polynomial function that belongs to the order-6 exponential-polynomial space $\mathcal{EP}^{\omega}_2$. The exponential-polynomial functions

$$\begin{aligned}
\phi^{\omega}_{0,2}(t) &= \frac{g_0(\omega-\omega t)}{g_0(\omega)},\\
\phi^{\omega}_{1,2}(t) &= g_1(\omega)\sinh\left(\frac{\omega}{2}\right)\left(\sinh^4\left(\frac{\omega-\omega t}{2}\right) - \sinh^4\left(\frac{\omega}{2}\right)\frac{g_0(\omega-\omega t)}{g_0(\omega)}\right),\\
\phi^{\omega}_{2,2}(t) &= g_2(\omega)\Bigg(-16\sinh^3\left(\frac{\omega-\omega t}{2}\right)\sinh\left(\frac{\omega t}{2}\right) + g_1(\omega)g_0(\omega)\sinh^4\left(\frac{\omega-\omega t}{2}\right)\\
&\qquad -g_1(\omega)\sinh^4\left(\frac{\omega}{2}\right)g_0(\omega-\omega t)\Bigg),\\
\phi^{\omega}_{3,2}(t) &= g_2(\omega)\Bigg(-16\sinh^3\left(\frac{\omega t}{2}\right)\sinh\left(\frac{\omega-\omega t}{2}\right) + g_1(\omega)g_0(\omega)\sinh^4\left(\frac{\omega t}{2}\right)\\
&\qquad -g_1(\omega)\sinh^4\left(\frac{\omega}{2}\right)g_0(\omega t)\Bigg),\\
\phi^{\omega}_{4,2}(t) &= g_1(\omega)\sinh\left(\frac{\omega}{2}\right)\left(\sinh^4\left(\frac{\omega t}{2}\right) - \sinh^4\left(\frac{\omega}{2}\right)\frac{g_0(\omega t)}{g_0(\omega)}\right),\\
\phi^{\omega}_{5,2}(t) &= \frac{g_0(\omega t)}{g_0(\omega)},
\end{aligned} \tag{4.2}$$

with

$$g_0(\omega) = 3\omega + \sinh(\omega)(\cosh(\omega)-4), \quad g_1(\omega) = \frac{4}{\sinh(\frac{\omega}{2})\left(\cosh(\omega) - 3\omega\coth(\frac{\omega}{2}) + 5\right)},$$

$$g_2(\omega) = \frac{\sinh(\frac{\omega}{2})}{3\big(3\sinh(\omega) - \omega(\cosh(\omega)+2)\big)},$$

Copyright © by SIAM. Unauthorized reproduction of this article is prohibited.

Downloaded 11/09/22 to 79.42.246.227 . Redistribution subject to SIAM license or copyright; see https://epubs.siam.org/terms-privacy

define a normalized B-basis of the extended Chebyshev space $\mathcal{EP}_2^\omega$ on $[0,1]$. For later use we observe that for the antiderivatives of the basis functions of $\mathcal{DEP}_2^\omega$ we can write

$$\begin{aligned}
&\int_0^t \varphi_{0,2}^\omega(x)dx = q_2(\omega)\ \sum_{i=1}^5 \phi_{i,2}^\omega(t), \quad \int_0^t \varphi_{1,2}^\omega(x)dx\ =\ q_3(\omega)\ \sum_{i=2}^5 \phi_{i,2}^\omega(t),\\
&\int_0^t \varphi_{2,2}^\omega(x)dx = \frac{q_4(\omega)}{q_1(\omega)}\ \sum_{i=3}^5 \phi_{i,2}^\omega(t),\\
&\int_0^t \varphi_{3,2}^\omega(x)dx = q_3(\omega)\ \sum_{i=4}^5 \phi_{i,2}^\omega(t), \quad \int_0^t \varphi_{4,2}^\omega(x)dx\ =\ q_2(\omega)\ \phi_{5,2}^\omega(t),
\end{aligned} \tag{4.3}$$

with

$$\begin{aligned}
q_2(\omega) &= \int_0^1 \varphi_{0,2}^\omega(t)\ dt = \frac{g_0(\omega)}{2\omega(\cosh(\omega)-1)^2},\\
q_3(\omega) &= \int_0^1 \varphi_{1,2}^\omega(t)\ dt = \frac{5\sinh(\omega)-3\omega+(\sinh(\omega)-3\omega)\cosh(\omega)}{\omega(\cosh(\omega)-1)^2},\\
q_4(\omega) &= q_1(\omega)\ \int_0^1 \varphi_{2,2}^\omega(t)\ dt = \frac{\omega(2+\cosh(\omega))-3\sinh(\omega)}{\omega(\cosh(\omega)-1)^2}.
\end{aligned} \tag{4.4}$$

Remark 4.1. For all $\omega \in \mathbb{R}^+$, we always have $g_0(\omega), g_1(\omega), g_2(\omega) \neq 0$ as well as $q_0(\omega), q_1(\omega), q_2(\omega), q_3(\omega), q_4(\omega) \neq 0$.

4.2. Geometric properties of Bézier-like curves in $\mathcal{EP}_2^\omega$.

DEFINITION 4.2 (Bézier-like curves in $\mathcal{EP}_2^\omega$). *Given a control polygon with vertices $\mathbf{r}_i \in \mathbb{R}^d$, $i = 0, \ldots, 5$, the associated Bézier-like curve in $\mathcal{EP}_2^\omega$ is defined as*

$$\mathbf{r}(t)\ =\ \sum_{i=0}^5 \mathbf{r}_i\, \phi_{i,2}^\omega(t), \qquad t \in [0,1]. \tag{4.5}$$

PROPOSITION 4.3 (properties of Bézier-like curves in $\mathcal{EP}_2^\omega$). *The Bézier-like curve in* (4.5) *has the following properties:*

(a) Convex hull property and geometric invariance property. *The entire curve lies inside the convex hull of its control points and its shape is independent of the coordinate system, i.e., it is scale and translation invariant.*

(b) Symmetry. *The control points* $\mathbf{r}_0, \mathbf{r}_1, \ldots, \mathbf{r}_5$ *and* $\mathbf{r}_5, \ldots, \mathbf{r}_1, \mathbf{r}_0$ *define the same curve with respect to different parameterizations, i.e.,*

$$\sum_{i=0}^5 \mathbf{r}_i \phi_{i,2}^\omega(t)\ =\ \sum_{i=0}^5 \mathbf{r}_{5-i} \phi_{i,2}^\omega(1-t), \qquad t \in [0,1].$$

(c) Derivative formula.

$$\frac{d}{dt}\mathbf{r}(t)\ =\ \sum_{i=0}^4 \frac{\Delta \mathbf{r}_i}{\int_0^1\ \varphi_{i,2}^\omega(x)\ dx}\, \varphi_{i,2}^\omega(t), \qquad t \in [0,1],$$

where, for all $i = 0, \ldots, 4$, $\Delta \mathbf{r}_i = \mathbf{r}_{i+1} - \mathbf{r}_i$.

Copyright © by SIAM. Unauthorized reproduction of this article is prohibited.

(d) Endpoint conditions.

$$\mathbf{r}(0) \;=\; \mathbf{r}_0, \qquad \mathbf{r}'(0) \;=\; \tfrac{1}{q_2(\omega)}(\mathbf{r}_1 - \mathbf{r}_0),$$

$$\mathbf{r}(1) \;=\; \mathbf{r}_5, \qquad \mathbf{r}'(1) \;=\; \tfrac{1}{q_2(\omega)}(\mathbf{r}_5 - \mathbf{r}_4).$$

Proof. See section SM5 for the proof. ∎

4.3. Control polygons of PH curves in $\mathcal{EP}_2^\omega$. To construct a spatial PH curve in $\mathcal{EP}_2^\omega$, the functions a_0, a_1, a_2, a_3 are chosen in $\mathcal{A}_2^\omega$ and thus $a_k(t) = \sum_{j=0}^{2} a_{k,j}\psi_{j,2}^\omega(t)$, $k \in \{0,\dots,3\}$, for some $a_{k,j} \in \mathbb{R}$. Consequently, the associated preimage is

$$\mathbf{A}(t) \;=\; \sum_{j=0}^{2} \mathbf{A}_j \psi_{j,2}^\omega(t), \tag{4.6}$$

where

$$\mathbf{A}_j \;=\; a_{0,j} \;+\; a_{1,j}\mathbf{i} \;+\; a_{2,j}\mathbf{j} \;+\; a_{3,j}\mathbf{k}, \qquad j = 0, 1, 2. \tag{4.7}$$

Proposition 4.4. *A PH curve $\mathbf{r}(t)$ in $\mathcal{EP}_2^\omega$ can be expressed in the Bézier-like form $\mathbf{r}(t) = \sum_{i=0}^{5} \mathbf{r}_i \phi_{i,2}^\omega(t)$, with Bézier-like control points $\mathbf{r}_i$, $i = 1,\dots,5$, given in terms of the freely chosen integration constant $\mathbf{r}_0$, of the numbers in* (4.1) *and* (4.4) *and of the coefficients of the preimage $\mathbf{A}(t)$ in* (4.6) *and* (4.7) *by*

$$\begin{aligned}
&\mathbf{r}_1 \;=\; \mathbf{r}_0 \;+\; q_2(\omega)\,\mathbf{A}_0\mathbf{i}\mathbf{A}_0^*, \qquad \mathbf{r}_2 \;=\; \mathbf{r}_1 \;+\; q_3(\omega)\,\frac{1}{2}\,(\mathbf{A}_0\mathbf{i}\mathbf{A}_1^* + \mathbf{A}_1\mathbf{i}\mathbf{A}_0^*),\\
&\mathbf{r}_3 \;=\; \mathbf{r}_2 \;+\; q_4(\omega)\,\left(\frac{1}{2}(\mathbf{A}_0\mathbf{i}\mathbf{A}_2^* + \mathbf{A}_2\mathbf{i}\mathbf{A}_0^*) + \frac{q_0(\omega)}{q_1(\omega)}\,\mathbf{A}_1\mathbf{i}\mathbf{A}_1^*\right),\\
&\mathbf{r}_4 \;=\; \mathbf{r}_3 \;+\; q_3(\omega)\,\frac{1}{2}\,(\mathbf{A}_1\mathbf{i}\mathbf{A}_2^* + \mathbf{A}_2\mathbf{i}\mathbf{A}_1^*), \qquad \mathbf{r}_5 \;=\; \mathbf{r}_4 \;+\; q_2(\omega)\,\mathbf{A}_2\mathbf{i}\mathbf{A}_2^*.
\end{aligned} \tag{4.8}$$

Proof. See section SM6 for the proof. ∎

Remark 4.5. Since, from (4.1) and (4.4),

$$\lim_{\omega\to 0} \frac{q_0(\omega)}{q_1(\omega)} \;=\; 2, \qquad \lim_{\omega\to 0} q_2(\omega) \;=\; \lim_{\omega\to 0} q_3(\omega) \;=\; \frac{1}{5}, \qquad \text{and} \qquad \lim_{\omega\to 0} q_4(\omega) \;=\; \frac{1}{15},$$

(4.8) recovers the well-known results of the quintic polynomial case when $\omega \to 0$; (see [3]).

4.4. Parametric speed and arc length in $\mathcal{EP}_2^\omega$.

Proposition 4.6. *The parametric speed of $\mathbf{r}(t)$ is a function in $\mathcal{DEP}_2^\omega$ having the expression $\sigma(t) = \sum_{i=0}^{4} \sigma_i \varphi_{i,2}^\omega(t)$, where*

$$\begin{aligned}
&\sigma_0 = |\mathbf{A}_0|^2, \qquad \sigma_1 \;=\; \frac{1}{2}(\mathbf{A}_1\mathbf{A}_0^* + \mathbf{A}_0\mathbf{A}_1^*),\\
&\sigma_2 = q_0(\omega)\,|\mathbf{A}_1|^2 \;+\; q_1(\omega)\,\frac{1}{2}\,(\mathbf{A}_2\mathbf{A}_0^* + \mathbf{A}_0\mathbf{A}_2^*),\\
&\sigma_3 = \frac{1}{2}(\mathbf{A}_1\mathbf{A}_2^* + \mathbf{A}_2\mathbf{A}_1^*), \qquad \sigma_4 \;=\; |\mathbf{A}_2|^2.
\end{aligned} \tag{4.9}$$

Proof. See section SM7 for the proof. ∎

Copyright © by SIAM. Unauthorized reproduction of this article is prohibited.

Downloaded 11/09/22 to 79.42.246.227 . Redistribution subject to SIAM license or copyright; see https://epubs.siam.org/terms-privacy

Downloaded 11/09/22 to 79.42.246.227 . Redistribution subject to SIAM license or copyright; see https://epubs.siam.org/terms-privacy

PROPOSITION 4.7. *The arc length function of* $\mathbf{r}(t)$ *is a function in* $\mathcal{EP}_2^\omega$ *having the expression* $s(t) = \sum_{i=0}^{5} s_i \phi_{i,2}^\omega(t)$, *where*

$$s_0 \;=\; 0, \qquad s_1 \;=\; s_0 \;+\; \sigma_0 q_2(\omega), \qquad s_2 \;=\; s_1 \;+\; \sigma_1 q_3(\omega),$$

$$s_3 \;=\; s_2 \;+\; \sigma_2 \frac{q_4(\omega)}{q_1(\omega)}, \qquad s_4 \;=\; s_3 \;+\; \sigma_3 q_3(\omega), \qquad s_5 \;=\; s_4 \;+\; \sigma_4 q_2(\omega).$$

Proof. See section SM8 for the proof. ∎

COROLLARY 4.8. *The total arc length of* $\mathbf{r}(t)$ *is*

$$\begin{aligned} s(1) = s_5 \;&=\; (\sigma_0+\sigma_4) q_2(\omega) \;+\; (\sigma_1+\sigma_3) q_3(\omega) \;+\; \sigma_2 \frac{q_4(\omega)}{q_1(\omega)} \\ &= q_2(\omega)\big(|\mathbf{A}_0|^2 + |\mathbf{A}_2|^2\big) + q_4(\omega)\frac{q_0(\omega)}{q_1(\omega)}|\mathbf{A}_1|^2 + q_3(\omega)\frac{1}{2}(\mathbf{A}_1\mathbf{A}_0^* + \mathbf{A}_0\mathbf{A}_1^*) \\ &\quad + q_3(\omega)\frac{1}{2}(\mathbf{A}_1\mathbf{A}_2^* + \mathbf{A}_2\mathbf{A}_1^*) + q_4(\omega)\,\frac{1}{2}\,(\mathbf{A}_2\mathbf{A}_0^* + \mathbf{A}_0\mathbf{A}_2^*). \end{aligned} \tag{4.10}$$

Remark 4.9. When $\omega \to 0$, the total arc length formula in (4.10) yields

$$\begin{aligned} s(1) = \frac{1}{5}\big(|\mathbf{A}_0|^2 + |\mathbf{A}_2|^2\big) \;+\; \frac{2}{15}|\mathbf{A}_1|^2 \;+\; \frac{1}{10}(\mathbf{A}_1\mathbf{A}_0^* + \mathbf{A}_0\mathbf{A}_1^*) \\ + \frac{1}{10}(\mathbf{A}_1\mathbf{A}_2^* + \mathbf{A}_2\mathbf{A}_1^*) \;+\; \frac{1}{30}(\mathbf{A}_2\mathbf{A}_0^* + \mathbf{A}_0\mathbf{A}_2^*), \end{aligned}$$

thus recovering the well-known result of the quintic polynomial case; (see [3]).

5. First-order Hermite interpolation by EPH curves. As in the polynomial case (see, e.g., [3, Chapter 28.1]), PH curves in $\mathcal{EP}_1^\omega$ could offer the possibility to interpolate G^1 Hermite data (i.e., endpoints and associated unit tangent vectors) at most. PH curves in $\mathcal{EP}_2^\omega$ are thus the simplest EPH curves that one could use to match C^1 Hermite data. The problem of interpolating C^1 Hermite data consists in constructing EPH curves that interpolate prescribed endpoints $\mathbf{r}_0$, $\mathbf{r}_5$ and first derivatives at these endpoints, hereinafter denoted by $\mathbf{d}_i$, $\mathbf{d}_f$, respectively. For the sake of conciseness, we also introduce the following abbreviations that do not specify the dependence on ω:

$$I_0 \;:=\; q_2(\omega), \qquad I_1 \;:=\; \frac{1}{2}q_3(\omega), \qquad I_2 \;:=\; \frac{1}{2}q_4(\omega), \qquad I_3 \;:=\; \frac{q_0(\omega)}{q_1(\omega)}\,q_4(\omega).$$

PROPOSITION 5.1. *The PH curves* $\mathbf{r}(t)$ *in* $\mathcal{EP}_2^\omega$ *solving the first-order Hermite interpolation problem* $\mathbf{r}(0) = \mathbf{r}_0$, $\mathbf{r}'(0) = \mathbf{d}_i$, $\mathbf{r}(1) = \mathbf{r}_5$, $\mathbf{r}'(1) = \mathbf{d}_f$, *have control points given by* (4.8) *with*

$$\begin{aligned} \mathbf{A}_0 \;&=\; \sqrt{|\mathbf{d}_i|}\,\frac{\mathbf{i}+\mathbf{w}_i}{|\mathbf{i}+\mathbf{w}_i|}\exp(\eta_0\mathbf{i}), \qquad \mathbf{A}_2 \;=\; \sqrt{|\mathbf{d}_f|}\,\frac{\mathbf{i}+\mathbf{w}_f}{|\mathbf{i}+\mathbf{w}_f|}\exp(\eta_2\mathbf{i}), \\ \mathbf{A}_1 \;&=\; -\frac{I_1}{I_3}(\mathbf{A}_0+\mathbf{A}_2) \;+\; \frac{\sqrt{|\mathbf{c}|}}{I_3}\,\frac{\mathbf{i}+\mathbf{w}_c}{|\mathbf{i}+\mathbf{w}_c|}\exp(\eta_1\mathbf{i}), \end{aligned} \tag{5.1}$$

where

$$\mathbf{c} \;:=\; I_3(\mathbf{r}_5-\mathbf{r}_0) \;+\; (I_1^2 - I_0 I_3)\,(\mathbf{d}_i+\mathbf{d}_f) \;+\; (I_1^2 - I_2 I_3)\,(\mathbf{A}_0\mathbf{i}\mathbf{A}_2^* + \mathbf{A}_2\mathbf{i}\mathbf{A}_0^*), \tag{5.2}$$

and

Copyright © by SIAM. Unauthorized reproduction of this article is prohibited.

- $(\lambda_i, \mu_i, \nu_i)$, $(\lambda_f, \mu_f, \nu_f)$, $(\lambda_c, \mu_c, \nu_c)$ *are the direction cosines of* $\mathbf{d}_i$, $\mathbf{d}_f$, *and* $\mathbf{c}$, *respectively;*
- $\mathbf{w}_i = \lambda_i\mathbf{i} + \mu_i\mathbf{j} + \nu_i\mathbf{k}$, $\mathbf{w}_f = \lambda_f\mathbf{i} + \mu_f\mathbf{j} + \nu_f\mathbf{k}$, $\mathbf{w}_c = \lambda_c\mathbf{i} + \mu_c\mathbf{j} + \nu_c\mathbf{k}$ *are unit vectors in the directions of* $\mathbf{d}_i$, $\mathbf{d}_f$, *and* $\mathbf{c}$, *respectively;*
- η_0, η_1, η_2 *are free angular variables in* $[-\pi/2, \pi/2]$.

Proof. In view of (2.5) and (4.6), interpolation of the end-derivatives yields the equations

$$\mathbf{A}_0\mathbf{i}\mathbf{A}_0^* = \mathbf{d}_i, \qquad \mathbf{A}_2\mathbf{i}\mathbf{A}_2^* = \mathbf{d}_f, \tag{5.3}$$

for $\mathbf{A}_0$ and $\mathbf{A}_2$, where $\mathbf{d}_i$ and $\mathbf{d}_f$ are known pure vector quaternions. Moreover, interpolation of the endpoints $\mathbf{r}_0$ and $\mathbf{r}_5$ gives the condition

$$\begin{aligned}\int_0^1 \mathbf{A}(t)\mathbf{i}\mathbf{A}^*(t)\,dt &= \mathbf{r}_5 - \mathbf{r}_0 \\ &= I_0\mathbf{A}_0\mathbf{i}\mathbf{A}_0^* + I_1(\mathbf{A}_0\mathbf{i}\mathbf{A}_1^* + \mathbf{A}_1\mathbf{i}\mathbf{A}_0^*) + I_2(\mathbf{A}_0\mathbf{i}\mathbf{A}_2^* + \mathbf{A}_2\mathbf{i}\mathbf{A}_0^*) \\ &\quad + I_3\mathbf{A}_1\mathbf{i}\mathbf{A}_1^* + I_1(\mathbf{A}_1\mathbf{i}\mathbf{A}_2^* + \mathbf{A}_2\mathbf{i}\mathbf{A}_1^*) + I_0\mathbf{A}_2\mathbf{i}\mathbf{A}_2^*.\end{aligned} \tag{5.4}$$

Recalling the result in [3, Chapter 28] and [4, section 3.2], the quaternion equations (5.3) can be solved directly obtaining

$$\mathbf{A}_0 = \sqrt{|\mathbf{d}_i|}\,\frac{\mathbf{i}+\mathbf{w}_i}{|\mathbf{i}+\mathbf{w}_i|}\exp(\eta_0\mathbf{i}) \qquad \text{and} \qquad \mathbf{A}_2 = \sqrt{|\mathbf{d}_f|}\,\frac{\mathbf{i}+\mathbf{w}_f}{|\mathbf{i}+\mathbf{w}_f|}\exp(\eta_2\mathbf{i}). \tag{5.5}$$

Knowing $\mathbf{A}_0$ and $\mathbf{A}_2$, the solution of (5.4) for $\mathbf{A}_1$ may appear more difficult. However, by using (5.3) and making appropriate rearrangements, (5.4) can be rewritten as

$$\begin{aligned}&(I_1\mathbf{A}_0 + I_3\mathbf{A}_1 + I_1\mathbf{A}_2)\mathbf{i}(I_1\mathbf{A}_0 + I_3\mathbf{A}_1 + I_1\mathbf{A}_2)^* = \\ &\quad = I_3(\mathbf{r}_5 - \mathbf{r}_0) + (I_1^2 - I_0I_3)(\mathbf{d}_i + \mathbf{d}_f) + (I_1^2 - I_2I_3)(\mathbf{A}_0\mathbf{i}\mathbf{A}_2^* + \mathbf{A}_2\mathbf{i}\mathbf{A}_0^*).\end{aligned} \tag{5.6}$$

Equation (5.6) is of the form $\widehat{\mathbf{A}}\mathbf{i}\widehat{\mathbf{A}}^* = \mathbf{c}$ (exactly as (5.3)) where

$$\widehat{\mathbf{A}} := I_1\mathbf{A}_0 + I_3\mathbf{A}_1 + I_1\mathbf{A}_2. \tag{5.7}$$

Note that $\mathbf{c}$ is a known pure vector quaternion. Exploiting (5.5) we can write

$$\mathbf{A}_0\mathbf{i}\mathbf{A}_2^* + \mathbf{A}_2\mathbf{i}\mathbf{A}_0^* = \sqrt{(1+\lambda_i)|\mathbf{d}_i|(1+\lambda_f)|\mathbf{d}_f|}(a_x\mathbf{i} + a_y\mathbf{j} + a_z\mathbf{k}),$$

where

$$\begin{aligned}a_x &= \cos(\Delta\eta) - \frac{(\mu_i\mu_f + \nu_i\nu_f)\cos(\Delta\eta) + (\mu_i\nu_f - \mu_f\nu_i)\sin(\Delta\eta)}{(1+\lambda_i)(1+\lambda_f)}, \\ a_y &= \frac{\mu_i\cos(\Delta\eta) - \nu_i\sin(\Delta\eta)}{1+\lambda_i} + \frac{\mu_f\cos(\Delta\eta) + \nu_f\sin(\Delta\eta)}{1+\lambda_f}, \\ a_z &= \frac{\nu_i\cos(\Delta\eta) + \mu_i\sin(\Delta\eta)}{1+\lambda_i} + \frac{\nu_f\cos(\Delta\eta) - \mu_f\sin(\Delta\eta)}{1+\lambda_f},\end{aligned}$$

with $\Delta\eta := \eta_2 - \eta_0$. Finally, writing $\mathbf{c} = c_x\mathbf{i} + c_y\mathbf{j} + c_z\mathbf{k}$, the solution of (5.6) for $\mathbf{A}_1$ is

$$\mathbf{A}_1 = -\frac{I_1}{I_3}(\mathbf{A}_0 + \mathbf{A}_2) + \frac{\sqrt{|\mathbf{c}|}}{I_3}\,\frac{\mathbf{i}+\mathbf{w}_c}{|\mathbf{i}+\mathbf{w}_c|}\exp(\eta_1\mathbf{i}),$$

which concludes the proof. ∎

Copyright © by SIAM. Unauthorized reproduction of this article is prohibited.

Downloaded 11/09/22 to 79.42.246.227 . Redistribution subject to SIAM license or copyright; see https://epubs.siam.org/terms-privacy

TABLE 2
All possible sign combinations of $\mathbf{A}_0$, $\mathbf{A}_1$, $\mathbf{A}_2$ *and their effects on the associated expressions.*

$\mathbf{A}_0$	$\mathbf{A}_1$	$\mathbf{A}_2$	$\mathbf{A}_0\mathbf{i}\mathbf{A}_1^* + \mathbf{A}_1\mathbf{i}\mathbf{A}_0^*$	$\mathbf{A}_0\mathbf{i}\mathbf{A}_2^* + \mathbf{A}_2\mathbf{i}\mathbf{A}_0^*$	$\mathbf{A}_1\mathbf{i}\mathbf{A}_2^* + \mathbf{A}_2\mathbf{i}\mathbf{A}_1^*$
+	+	+	+	+	+
+	+	-	+	-	-
+	-	+	-	+	-
+	-	-	-	-	+
-	+	+	-	-	+
-	+	-	-	+	-
-	-	+	+	-	-
-	-	-	+	+	+

Remark 5.2. When $\omega \to 0$ the result of Proposition 5.1 gets back the well-known result of the quintic polynomial case treated in [4].

Remark 5.3. The three angular variables η_0, η_1, η_2, associated with the quaternions $\mathbf{A}_0$, $\mathbf{A}_1$, $\mathbf{A}_2$ respectively, do not identify independent degrees of freedom. Indeed, the control points of spatial EPH Hermite interpolants depend only on ω and the difference of the angles η_0, η_1, η_2. Thus, without loss of generality, we can assume η_1 to be fixed and, by introducing the notation $\Delta\eta = \eta_2 - \eta_0$ and $\eta_m = (\eta_0 + \eta_2)/2$, write $\eta_0 = \eta_m - \Delta\eta/2$, $\eta_2 = \eta_m + \Delta\eta/2$. Moreover, while the choice $\eta_k \in [-\pi/2, \pi/2]$, $k \in \{0, 1, 2\}$, covers all possible different solutions of the Hermite interpolation problem, these are also recovered by the choice $\eta_k \in [0, \pi]$, $k \in \{0, 1, 2\}$. Indeed, if we substitute $\mathbf{A}_k$ with $\mathbf{A}_k\mathbf{i}$, $k \in \{0, 1, 2\}$, in (4.8) we obtain exactly the same control points. However, doing so, (5.1) has to be multiplied from the right by $\mathbf{i}$, which leads to $\exp((\eta_k + \pi/2)\mathbf{i})$ instead of $\exp(\eta_k\mathbf{i})$, $k \in \{0, 1, 2\}$.

Remark 5.4. As already observed, to recover the result for the planar case with $a_0(t) = a_3(t) = 0$, we need to have $\mathbf{A}_0, \mathbf{A}_1, \mathbf{A}_2 \in \text{span}\{\mathbf{i}, \mathbf{j}\}$. Therefore we must have $\eta_0, \eta_1, \eta_2 \in \{0, \pi\}$ (see Remark 5.3). Even if the possible combinations of η_k, $k \in \{0, 1, 2\}$, are eight, due to (4.8) we obtain only four different curves. Indeed, if we reason on the signs of $\mathbf{A}_k$, $k \in \{0, 1, 2\}$, we get the results collected in Table 2. Thus, as stated in Remark 5.3, one can obtain the four different planar Hermite interpolants by fixing $\eta_1 = 0$ and then choosing $\eta_0, \eta_2 \in \{0, \pi\}$. Since fixing $\eta_1 = 0$ means taking $\mathbf{A}_1$ with the sign +, we refer to the four possible planar solutions with the notation $++$, $+-$, $-+$, $--$ to specify the four possible combinations of the signs of $\mathbf{A}_0$ and $\mathbf{A}_2$ that one could consider.

Figure 2 shows, in the second row, an application of Proposition 5.1 for planar Hermite data, while an application for spatial Hermite data is illustrated in Figure 4.

6. Evaluation of EPH curves. In order to evaluate EPH curves two considerations have to be done. On the one hand, looking at the expressions of the normalized B-basis 3.4 and 4.2, it is clear that they are not suited for computations when ω is large. The strategy to avoid this problem is to express all the functions involved as a ratio of exponential polynomials, simplifying the dominant growth term. Unfortunately, the resulting expressions are very long. For this reason they are not presented here, but they can be found in section SM10.

On the other hand, computational problems also arise for small values of ω. Unfortunately, this issue cannot be solved like the previous one with an analytic trick. A way to proceed in this case is to consider for each basis function $\phi_{i,m}^{\omega}(t)$ its corresponding Taylor expansion $T_{i,m}^{\omega}(t)$ at $\omega = 0$ up to a certain order, and then to rely on an efficient algorithm for polynomial evaluation. This is a fair strategy, even

Copyright © by SIAM. Unauthorized reproduction of this article is prohibited.

Downloaded 11/09/22 to 79.42.246.227 . Redistribution subject to SIAM license or copyright; see https://epubs.siam.org/terms-privacy

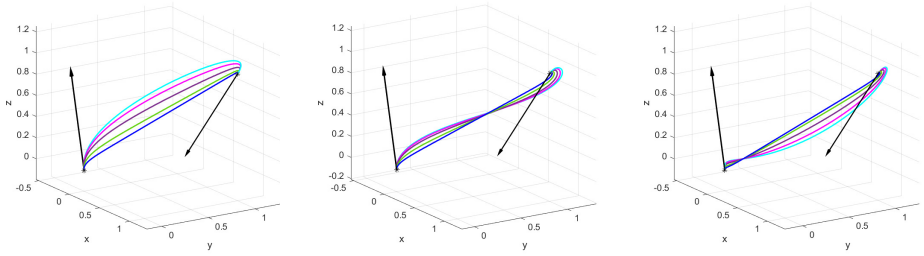

FIG. 4. *One-parameter families of spatial EPH Hermite interpolants to the data* $\mathbf{r}_0 = (0,0,0)$, $\mathbf{r}_5 = (1,1,1)$, $\mathbf{d}_i = (-0.8, 0.3, 1.2)$, $\mathbf{d}_f = (0.5, -1.3, -1)$, *defined by fixing* $\eta_1 = -\pi/2$, $\Delta\eta = \pi/3$ *and* $\eta_m = -\pi/2$ *(left),* $\eta_m = -\pi/10$ *(center),* $\eta_m = 3\pi/10$ *(right). The family members of each subfigure are obtained with* $\omega \in \{0.1, 3, 6, 12, 24\}$, *where a bigger value of* ω *results in a straighter curve connecting the two endpoints.*

from a theoretical point of view, since, for $\omega \to 0$, the considered EPH spaces become exactly polynomial spaces. In our numerical computations we considered fifth-order Taylor expansions which, for completeness, can be found in section SM9.

Here we propose a new ad hoc pointwise evaluation algorithm and we compare it with the de Casteljau–like B-algorithm [7] and the recent method proposed by Woźny and Chudy in [13]. For the sake of brevity, we only provide a sketch of these two algorithms in Algorithms 6.1 and 6.2, where the auxiliary functions $\lambda^{\omega}_{i,j,m}$ and $h^{\omega}_{j,m}$ are constructed following the strategies detailed in [7] and [13], respectively. In order to implement the methods, we recall that all the functions involved must be rewritten in a stable form as the basis functions in section SM10.

Each of these methods has a different running time and a different behavior as ω approaches 0. As shown in this section, the newly proposed algorithm yields the best results on both fronts and therefore we suggest it as the go-to evaluation algorithm for EPH curves.

We recall that, fixed $d \in \{2,3\}$ and $m \in \{1,2\}$, our interest here is to evaluate the curve $\mathbf{r}(t) = \sum_{i=0}^{2m+1} \mathbf{r}_i \phi^{\omega}_{i,m}(t)$, at a given $\hat{t} \in [0,1]$, for a set of control points $\mathbf{r}_i \in \mathbb{R}^d$, $i = 0, \ldots, 2m+1$. The de Casteljau's algorithm finds the value of $\mathbf{r}(\hat{t})$ computing recursively $2m+1$ new sets of points, $\{\mathbf{r}^k_i\}_{i=0}^{2m+1-k}$, $k = 1, \ldots, 2m+1$, each having one

Algorithm 6.1 de Casteljau–like

Acquire $\mathbf{r}^0_0 := \mathbf{r}_0,\ \mathbf{r}^0_1 := \mathbf{r}_1,\ \ldots,\ \mathbf{r}^0_{2m+1} := \mathbf{r}_{2m+1},\ \hat{t}$
for $k = 1, \ldots, 2m+1$ **do**
  for $i = 0, \ldots, 2m+1-k$ **do**
    $\mathbf{r}^k_i \longleftarrow (1 - \lambda^{\omega}_{i,2m+1-k,m}(\hat{t}))\, \mathbf{r}^{k-1}_i + \lambda^{\omega}_{i,2m+1-k,m}(\hat{t}) \mathbf{r}^{k-1}_{i+1}$
  end for
end for
return $\mathbf{r}^{2m+1}_0$

Algorithm 6.2 Woźny–Chudy

Acquire $\mathbf{q}_0 := \mathbf{r}_0,\ \mathbf{r}_1,\ \ldots,\ \mathbf{r}_{2m+1},\ \hat{t}$
for $k = 1, \ldots, 2m+1$ **do**
  $\mathbf{q}_k \longleftarrow (1 - h^{\omega}_{2m+1-k,m}(\hat{t}))\, \mathbf{q}_{k-1} + h^{\omega}_{2m+1-k,m}(\hat{t}) \mathbf{r}_k$
end for
return $\mathbf{q}_{2m+1}$

Copyright © by SIAM. Unauthorized reproduction of this article is prohibited.

Downloaded 11/09/22 to 79.42.246.227 . Redistribution subject to SIAM license or copyright; see https://epubs.siam.org/terms-privacy

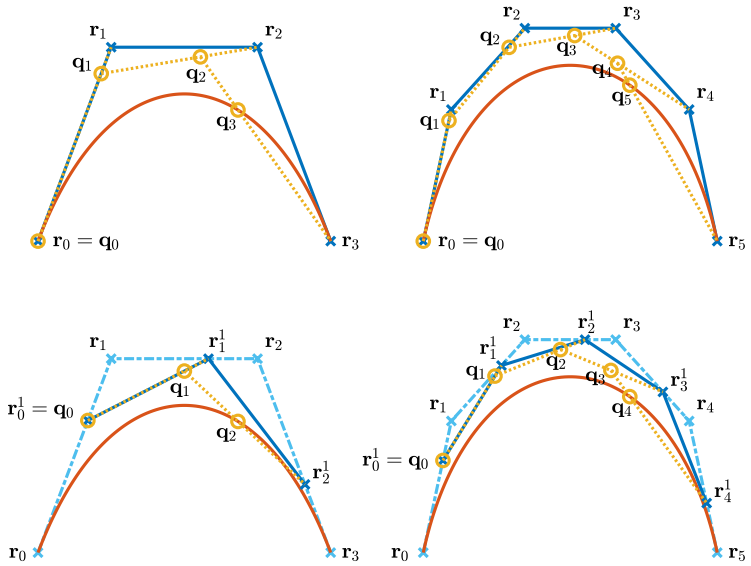

FIG. 5. *Geometrical comparison between the Woźny–Chudy evaluation algorithm (first row) and the new proposed method (second row) when applied to a curve in* $\mathcal{EP}_1^\omega$ *(first column) and a curve in* $\mathcal{EP}_2^\omega$ *(second column).*

point less than the previous one. At each level k, the new set of points is obtained as a convex combination of two consecutive points in the previous level. Instead of computing smaller and smaller sets of control points, Woźny and Chudy's method consists in $2m+1$ convex combinations, each of them adding the contribution of one of the initial control points. A graphical layout of the algorithm can be seen in the first row of Figure 5.

The new algorithm hereby proposed somehow combines the approaches of both de Casteljau and Woźny–Chudy. The idea is to first compute a new set of control vertices, $\{\mathbf{r}_i^1\}_{i=0}^{2m}$, starting from the initial control points, similar to a de Casteljau step. These new vertices are computed such that the associated polynomial Bézier curve of degree $2m$ has the same evaluation as $\mathbf{r}(t)$ at the desired point $\hat{t} \in (0,1)$, i.e., $\mathbf{r}(\hat{t}) = \sum_{i=0}^{2m} \mathbf{r}_i^1 B_{i,2m}(\hat{t})$ with $B_{i,2m}(\hat{t}) = \binom{2m}{i} \hat{t}^i (1-\hat{t})^{2m-i}$, where the right-hand side can be efficiently computed via Woźny–Chudy for polynomial curves, which is much faster than its specialized version for EPH curves. The detailed steps of the method are described in Algorithm 6.3, where, for $m = 1$,

$$\tau_{0,1}^\omega(t) = \frac{\phi_{0,1}^\omega(t)}{(1-t)^2}, \qquad \tau_{2,1}^\omega(t) = 1 - \frac{\phi_{3,1}^\omega(t)}{t^2},$$

$$\tau_{1,1}^\omega(t) = \frac{\phi_{0,1}^\omega(t) + \phi_{1,1}^\omega(t) - (1-t)^2}{2t(1-t)} = 1 - \frac{\phi_{2,1}^\omega(t) + \phi_{3,1}^\omega(t) - t^2}{2t(1-t)},$$

and, for $m = 2$,

$$\tau_{0,2}^\omega(t) = \frac{\phi_{0,2}^\omega(t)}{(1-t)^4}, \qquad \tau_{1,2}^\omega(t) = \frac{\phi_{0,2}^\omega(t) + \phi_{1,2}^\omega(t) - (1-t)^4}{4t(1-t)^3},$$

$$\tau_{2,2}^\omega(t) = \frac{\sum_{i=0}^{2} \phi_{i,2}^\omega(t) - (1-t)^4 - 4t(1-t)^3}{6t^2(1-t)^2} = 1 - \frac{\sum_{i=3}^{5} \phi_{i,2}^\omega(t) - 4t^3(1-t) - t^4}{6t^2(1-t)^2},$$

$$\tau_{3,2}^\omega(t) = 1 - \frac{\phi_{4,2}^\omega(t) + \phi_{5,2}^\omega(t) - t^4}{4t^3(1-t)}, \qquad \tau_{4,2}^\omega(t) = 1 - \frac{\phi_{5,2}^\omega(t)}{t^4}.$$

Copyright © by SIAM. Unauthorized reproduction of this article is prohibited.

Downloaded 11/09/22 to 79.42.246.227 . Redistribution subject to SIAM license or copyright; see https://epubs.siam.org/terms-privacy

Algorithm 6.3 New proposal

Acquire $\mathbf{r}_0, \ldots, \mathbf{r}_{2m+1}, \hat{t}$
if $\hat{t} = 0$ **then**
  return $\mathbf{r}_0$
else if $\hat{t} = 1$ **then**
  return $\mathbf{r}_{2m+1}$
else
  for $j = 0, \ldots, 2m$ **do**
    $\mathbf{r}_j^1 \longleftarrow \tau_{j,m}^{\omega}(\hat{t})\mathbf{r}_j + \big(1 - \tau_{j,m}^{\omega}(\hat{t})\big)\mathbf{r}_{j+1}$
  end for
  if $\hat{t} \in [0.5, 1)$ **then**
    $\mathbf{q}_0 \longleftarrow \mathbf{r}_0^1, \quad h_0 \longleftarrow 1 \quad \text{and} \quad D \longleftarrow \frac{1-\hat{t}}{\hat{t}}$
    for $k = 1, \ldots, 2m$ **do**
      $h_k \longleftarrow \left(1 + \frac{kD}{(2m+1-k)h_{k-1}}\right)^{-1} \quad \text{and} \quad \mathbf{q}_k \longleftarrow (1 - h_k)\,\mathbf{q}_{k-1} + h_k \mathbf{r}_k^1$
    end for
  else if $\hat{t} \in (0, 0.5)$ **then**
    $\mathbf{q}_0 \longleftarrow \mathbf{r}_{2m}^1, \quad h_0 \longleftarrow 1 \quad \text{and} \quad D \longleftarrow \frac{\hat{t}}{1-\hat{t}}$
    for $k = 1, \ldots, 2m$ **do**
      $h_k \longleftarrow \left(1 + \frac{kD}{(2m+1-k)h_{k-1}}\right)^{-1} \quad \text{and} \quad \mathbf{q}_k \longleftarrow (1 - h_k)\,\mathbf{q}_{k-1} + h_k \mathbf{r}_{2m-k}^1$
    end for
  end if
  return $\mathbf{q}_{2m}$
end if

As for the basis functions, the stable expressions for $\{\tau_{j,m}^{\omega}(t)\}_{j=0}^{2m}$ exploited in our implementation can be found in section SM11. A graphical layout of the algorithm can be seen in the second row of Figure 5.

Remark 6.1. The functions $\tau_{j,m}^{\omega}(\hat{t})$ have removable discontinuities in $\hat{t} = 0$ and $\hat{t} = 1$. These are bypassed by the first two "if"s in Algorithm 6.3. In theory, one should be careful to evaluate for $\hat{t}$ close to 0 or 1, e.g., approximating each $\tau_{j,m}^{\omega}(\hat{t})$ with its truncated Taylor expansion. In practice, while using MATLAB, problems occur only for values of $\hat{t}$ which are extremely close to 0 and 1. For instance, evaluation of PH curves in $\mathcal{EP}_2^{\omega}$ for values of $\hat{t}$ close to 0 starts giving problems at $\hat{t} \approx 10^{-80}$. Since this limitation does not affect its practical use, for the sake of simplicity, Algorithm 6.3 does not include any modification to handle that situation.

6.1. Comparing the three evaluation methods. We start comparing the behavior of the three methods as ω goes to 0. In order to do so, we computed, for 500 equispaced values of $\omega \in (0, 2]$, the maximum over 100 curves with random control points uniformly distributed in $(0, 1)^d$ of the relative error in the infinity norm committed by each method in approximating the fifth-order Taylor expansion of the curve at $\omega = 0$. In other words, in Figure 6, one can see, for $d = 3$ and $m \in \{1, 2\}$, the behavior of the function

$$\rho_{d,m}(\omega) := \max_{\{\mathbf{r}_i\}_{i=0}^{2m+1} \in \mathcal{R}} \frac{\left\| \sum_{i=0}^{2m+1} \mathbf{r}_i T_{i,m}^{\omega}(t)\Big|_{\mathbf{z}} - \sum_{i=0}^{2m+1} \mathbf{r}_i \phi_{i,m}^{\omega}(t)\Big|_{\mathbf{z}} \right\|_{\infty}}{\left\| \sum_{i=0}^{2m+1} \mathbf{r}_i T_{i,m}^{\omega}(t)\Big|_{\mathbf{z}} \right\|_{\infty}}, \tag{6.1}$$

Copyright © by SIAM. Unauthorized reproduction of this article is prohibited.

Downloaded 11/09/22 to 79.42.246.227 . Redistribution subject to SIAM license or copyright; see https://epubs.siam.org/terms-privacy

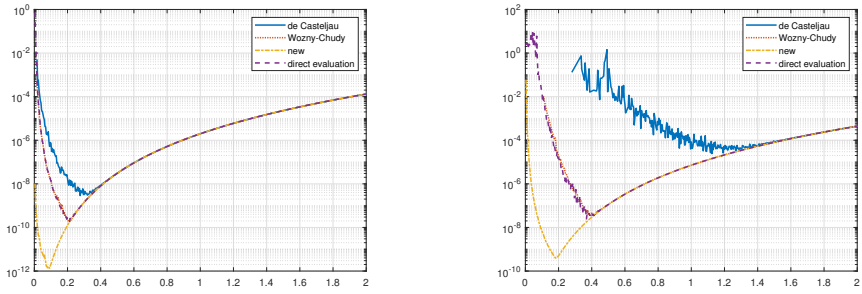

FIG. 6. *The function $\rho_{d,m}(\omega)$ in (6.1) for $d = 3$ and $m \in \{1, 2\}$ computed with three different methods (the de Casteljau–like B-algorithm, the Woźny–Chudy algorithm, and the new proposed method) and using the direct evaluation of (3.4) and (4.2) as a benchmark.*

TABLE 3
Estimated $\overline{\omega} = \operatorname{argmin}_{\omega \in (0,2]} \rho_{d,m}(\omega)$ for $\rho_{d,m}(\omega)$ in (6.1) with $d = 3$ and $m \in \{1, 2\}$ for the three considered methods and the direct evaluation of (3.4) and (4.2) as a benchmark.

m	de Casteljau–like	Woźny–Chudy	New proposal	Direct evaluation
1	0.2760	0.2200	0.0960	0.2120
2	1.1160	0.3800	0.1840	0.3680

where $\mathcal{R}$ is a collection of 100 random sets of $2m + 2$ control points in $(0, 1)^d$, $\mathbf{z} = [k/500]_{k=0}^{500}$, and $\sum_{i=0}^{2m+1} \mathbf{r}_i \phi_{i,m}^{\omega}(t)\big|_{\mathbf{z}}$ is computed with each of the three considered methods. From a theoretical point of view, as ω gets closer and closer to 0, an exact evaluation of the curve should approach the evaluation of the polynomial curve obtained substituting each basis function $\phi_{i,m}^{\omega}$ with its corresponding Taylor polynomial, and thus we should get $\rho_{d,m}(\omega) \to 0$ for $\omega \to 0$. Since stability for small ω is not achievable, we have that, for each method, the value of $\rho_{d,m}(\omega)$ decreases until a certain threshold is met, under which $\rho_{d,m}(\omega)$ starts to increase and the method becomes unreliable. In particular, from Figure 6 it is possible to see how the newly proposed algorithm is the one that can get the closest to 0 without having numerical issues. For the sake of completeness the points of minimum found for each graph are reported in Table 3. Therefore, the proposed method is the one that allows exact evaluation for the largest subset of $\omega \in \mathbb{R}^+$.

Concerning the running time of the three algorithms, fixed $d = 3$ and $m \in \{1, 2\}$, for each $\omega \in \{0.0960 + 2^k\}_{k=-50}^{50}$ we evaluated 10000 random curves at 501 equispaced points in $[0, 1]$. The results are visible in Figure 7, where again the new proposed algorithm is the best performing one in both scenarios and for every value of ω we considered. We observe that the slope around $\omega = 10^3$ is due to the fact that most of the exponential functions involved in the computations become very small and thus are set to 0, speeding up most computations. All numerical experiments were done in MATLAB 2021b on a laptop equipped with an Intel Core i7-10870H CPU and 32 GB RAM.

6.2. A note on a fourth algorithm. We conclude this section with a short discussion about the dynamic evaluation algorithm presented in [14, 15] which, although it can be specialized for EPH curves, presents stability issues for large values of ω. To explain why this is the case, we begin with a brief review of the method. First, it must be that $\det([\mathbf{r}_{2m-d+2}, \ldots, \mathbf{r}_{2m+1}]) \neq 0$. Then the method evaluates $\mathbf{r}(t)$ in $k \in \mathbb{N} \setminus \{1\}$ equispaced points over $[0, 1]$, finding $\mathbf{y}_i = \mathbf{r}(ih) \in \mathbb{R}^d$, $i = 0, \ldots, k - 1$,

Copyright © by SIAM. Unauthorized reproduction of this article is prohibited.

Downloaded 11/09/22 to 79.42.246.227 . Redistribution subject to SIAM license or copyright; see https://epubs.siam.org/terms-privacy

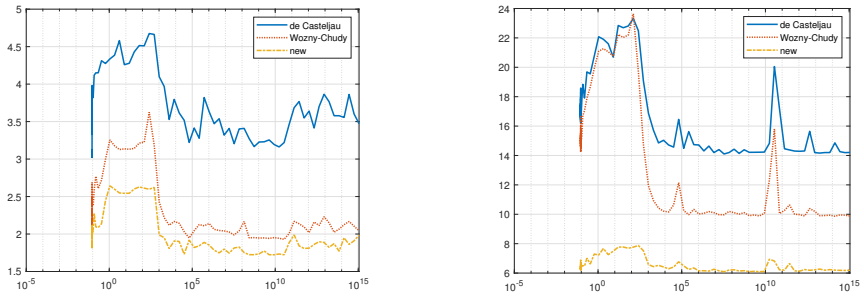

$m = 1$ $m = 2$

FIG. 7. *Running times in seconds of the three considered methods for the evaluation of* 10000 *random curves, varying* ω *in* $\{0.0920 + 2^k\}_{k=-50}^{50}$*, for* $d = 3$ *and* $m \in \{1, 2\}$.

where $h = 1/(k-1)$. Once the matrices $\mathbf{R}_1 := [\mathbf{r}_0, \dots, \mathbf{r}_{2m-d+1}] \in \mathbb{R}^{d\times(2m-d+2)}$ and $\mathbf{R}_2 := [\mathbf{r}_{2m-d+2}, \dots, \mathbf{r}_{2m+1}] \in \mathbb{R}^{d\times d}$ are defined, the problem is lifted to dimension $2m+2$, where the new control points are the columns of $\mathbf{R} := \left[\begin{smallmatrix} \mathbf{R}_1, & \mathbf{R}_2 \\ \mathbf{I}_{2m-d+2}, & \mathbf{O}_{(2m-d+2)\times d} \end{smallmatrix}\right] \in \mathbb{R}^{(2m+2)\times(2m+2)}$, where $\mathbf{I}_{2m-d+2}$ is the $(2m-d+2)$-dimensional identity matrix and $\mathbf{O}_{(2m-d+2)\times d}$ is the $(2m-d+2)\times d$ matrix of zeros. It is easy to see that $\mathbf{R}$ is invertible with $\mathbf{R}^{-1} = \left[\begin{smallmatrix} \mathbf{O}_{(2m-d+2)\times d}, & \mathbf{I}_{2m-d+2} \\ \mathbf{R}_2^{-1}, & \mathbf{R}_2^{-1}\,\mathbf{R}_1 \end{smallmatrix}\right]$. Now consider the following recursion:

$$\mathbf{z}_0 \;=\; \mathbf{R}\,\mathbf{e}_1, \qquad \mathbf{z}_i \;=\; \mathbf{M}\,\mathbf{z}_{i-1} \;=\; \mathbf{M}^i\,\mathbf{z}_0, \qquad i = 1, \dots, k-1, \tag{6.2}$$

where $\mathbf{e}_1 = [\delta_{1,j}]_{j=1}^{2m+2}$, $\delta_{i,j}$ being the Kronecker delta, $\mathbf{M} = \mathbf{R}\mathbf{C}_{h,m}^{\omega}\mathbf{R}^{-1}$, and $\mathbf{C}_{h,m}^{\omega} \in \mathbb{R}^{(2m+2)\times(2m+2)}$ is the unique matrix such that

$$\begin{bmatrix} \phi_{0,m}^{\omega}(t+h) \\ \vdots \\ \phi_{2m+1,m}^{\omega}(t+h) \end{bmatrix} \;=\; \mathbf{C}_{h,m}^{\omega} \begin{bmatrix} \phi_{0,m}^{\omega}(t) \\ \vdots \\ \phi_{2m+1,m}^{\omega}(t) \end{bmatrix}, \qquad 0 \le t+h \le 1,\ t \in [0,1].$$

Then $\mathbf{y}_i = \begin{bmatrix} \mathbf{I}_d, & \mathbf{O}_{d\times(2m+2)} \end{bmatrix} \mathbf{z}_i$, $i = 0, \dots, k-1$. In other words, once we have the evaluations of the lifted curve $\{\mathbf{z}_i\}_{i=0}^{k-1}$, we only need to consider the first d components to find the solution for the initial low-dimensional problem.

Let us now focus on the space $\mathcal{EP}_1^{\omega}$. To use the previous method we need to compute the matrix $\mathbf{C}_{h,1}^{\omega}$. Since

$$\mathbf{B}\begin{bmatrix} \phi_{0,1}^{\omega}(t) \\ \phi_{1,1}^{\omega}(t) \\ \phi_{2,1}^{\omega}(t) \\ \phi_{3,1}^{\omega}(t) \end{bmatrix} \;=\; \begin{bmatrix} 1 \\ t \\ e^{\omega t} \\ e^{-\omega t} \end{bmatrix} \quad \text{with} \quad \mathbf{B} \;=\; \begin{bmatrix} 1 & 1 & 1 & 1 \\ 0 & c_2(\omega) & 1-c_2(\omega) & 1 \\ 1 & 1+\omega c_2(\omega) & e^{\omega}(1-\omega c_2(\omega)) & e^{\omega} \\ 1 & 1-\omega c_2(\omega) & e^{-\omega}(1+\omega c_2(\omega)) & e^{-\omega} \end{bmatrix}$$

and

$$\begin{bmatrix} 1 \\ t+h \\ e^{\omega(t+h)} \\ e^{-\omega(t+h)} \end{bmatrix} \;=\; \widehat{\mathbf{C}}_{h,1}^{\omega} \begin{bmatrix} 1 \\ t \\ e^{\omega t} \\ e^{-\omega t} \end{bmatrix} \qquad \text{with} \qquad \widehat{\mathbf{C}}_{h,1}^{\omega} \;=\; \begin{bmatrix} 1 & 0 & 0 & 0 \\ h & 1 & 0 & 0 \\ 0 & 0 & e^{\omega h} & 0 \\ 0 & 0 & 0 & e^{-\omega h} \end{bmatrix},$$

we have that

$$\begin{bmatrix} \phi_{0,1}^{\omega}(t+h) \\ \phi_{1,1}^{\omega}(t+h) \\ \phi_{2,1}^{\omega}(t+h) \\ \phi_{3,1}^{\omega}(t+h) \end{bmatrix} \;=\; \mathbf{C}_{h,1}^{\omega} \begin{bmatrix} \phi_{0,1}^{\omega}(t) \\ \phi_{1,1}^{\omega}(t) \\ \phi_{2,1}^{\omega}(t) \\ \phi_{3,1}^{\omega}(t) \end{bmatrix} \qquad \text{with} \qquad \mathbf{C}_{h,1}^{\omega} \;=\; \mathbf{B}^{-1}\,\widehat{\mathbf{C}}_{h,1}^{\omega}\,\mathbf{B}.$$

Copyright © by SIAM. Unauthorized reproduction of this article is prohibited.

Downloaded 11/09/22 to 79.42.246.227 . Redistribution subject to SIAM license or copyright; see https://epubs.siam.org/terms-privacy

In particular, it can be shown that

$$\mathbf{C}^{\omega}_{h,1}(4,4) = \frac{\sinh(\omega(1+h)) \ - \ \omega(1+h)}{\sinh(\omega) \ - \ \omega} \ = \ \frac{e^{\omega(1+h)} \ - \ e^{-\omega(1+h)} \ - \ 2\omega(1+h)}{e^{\omega} \ - \ e^{-\omega} \ - \ 2\omega}$$
$$= e^{\omega h} \ \frac{1 \ - \ e^{-2\omega(1+h)} \ - \ 2\omega e^{-\omega(1+h)}}{1 \ - \ e^{-2\omega} \ - \ 2\omega e^{-\omega}} \ = \ \mathcal{O}(e^{\omega h}) \qquad \text{for} \qquad \omega \to +\infty,$$

since $h \in (0, 1]$. This fact propagates to $\mathbf{M}$ and its powers during the recursion (6.2) which ends with $\mathbf{M}^{k-1}$ having an element that is $\mathcal{O}(e^{\omega})$, making the computations numerically unstable already for ω of order 10^1. In a similar way it is possible to check that the same happens for the space $\mathcal{EP}^{\omega}_2$. Thus, it is not advisable to use this evaluation method in the context here described.

Acknowledgments. This work has been accomplished within the "Research ITalian network on Approximation" (RITA) and the TAA-UMI group.

REFERENCES

[1] J. M. Carnicer and J. M. Peña, *Totally positive bases for shape preserving curve design and optimality of B-splines*, Comput. Aided Geom. Design, 11 (1994), pp. 633–654, https://doi.org/10.1016/0167-8396(94)90056-6.

[2] I. Cattiaux-Huillard and L. Saini, *Characterization and extensive study of cubic and quintic algebraic trigonometric planar PH curves*, Adv. Comput. Math., 46 (2020), https://doi.org/10.1007/s10444-020-09772-4.

[3] R. T. Farouki, *Pythagorean-Hodograph Curves: Algebra and Geometry Inseparable*, Geom. Comput. 2, Springer, Berlin, 2008, https://doi.org/10.1007/978-3-540-73398-0.

[4] R. T. Farouki, M. al Kandari, and T. Sakkalis, *Hermite interpolation by rotation-invariant spatial Pythagorean-hodograph curves*, Adv. Comput. Math., 17 (2002), pp. 369–383, https://doi.org/10.1023/A:1016280811626.

[5] C. González, G. Albrecht, M. Paluszny, and M. Lentini, *Design of C^2 algebraic-trigonometric pythagorean hodograph splines with shape parameters*, Comput. Appl. Math., 37 (2018), pp. 1472–1495, https://doi.org/10.1007/s40314-016-0404-y.

[6] J. Kozak, M. Krajnc, M. Rogina, and V. Vitrih, *Pythagorean-hodograph cycloidal curves*, J. Numer. Math., 23 (2015), pp. 345–360, https://doi.org/10.1515/jnma-2015-0023.

[7] E. Mainar and J. M. Peña, *Corner cutting algorithms associated with optimal shape preserving representations*, Comput. Aided Geom. Design, 16 (1999), pp. 883–906, https://doi.org/10.1016/S0167-8396(99)00035-7.

[8] E. Mainar and J. M. Peña, *A general class of Bernstein-like bases*, Comput. Math. Appl., 53 (2007), pp. 1686–1703, https://doi.org/10.1016/j.camwa.2006.12.018.

[9] E. Mainar and J. M. Peña, *Optimal bases for a class of mixed spaces and their associated spline spaces*, Comput. Math. Appl., 59 (2010), pp. 1509–1523, https://doi.org/10.1016/j.camwa.2009.11.009.

[10] L. Romani and F. Montagner, *Algebraic-trigonometric Pythagorean-hodograph space curves*, Adv. Comput. Math., 45 (2019), pp. 75–98, https://doi.org/10.1007/s10444-018-9606-8.

[11] L. Romani, L. Saini, and G. Albrecht, *Algebraic-trigonometric Pythagorean-hodograph curves and their use for Hermite interpolation*, Adv. Comput. Math., 40 (2014), pp. 977–1010, https://doi.org/10.1007/s10444-013-9338-8.

[12] A. Róth, *Algorithm 992: an OpenGL- and C++-based function library for curve and surface modeling in a large class of extended Chebyshev spaces*, ACM Trans. Math. Software, 45 (2019), https://doi.org/10.1145/3284979.

[13] P. Woźny and F. Chudy, *Linear-time geometric algorithm for evaluating Bézier curves*, Comput.-Aided Des., 118 (2020), 102760, https://doi.org/10.1016/j.cad.2019.102760.

[14] X. Yang and J. Hong, *Dynamic evaluation of free-form curves and surfaces*, SIAM J. Sci. Comput., 39 (2017), pp. B424–B441, https://doi.org/10.1137/16M1058911.

[15] X. Yang and J. Hong, *Dynamic evaluation of exponential polynomial curves and surfaces via basis transformation*, SIAM J. Sci. Comput., 41 (2019), pp. A3401–A3420, https://doi.org/10.1137/18M1230359.

Copyright © by SIAM. Unauthorized reproduction of this article is prohibited.

Downloaded 11/09/22 to 79.42.246.227 . Redistribution subject to SIAM license or copyright; see https://epubs.siam.org/terms-privacy